Rev Physiol Biochem Pharmacol (2006)
DOI 10.1007/112_0603

S. C. Sinha · S. R. Sprang

Structures, mechanism, regulation and evolution of class III nucleotidyl cyclases

Published online: 12 September 2006

Abstract Cyclic 3′,5′-guanylyl and adenylyl nucleotides function as second messengers in eukaryotic signal transduction pathways and as sensory transducers in prokaryotes. The nucleotidyl cyclases (NCs) that catalyze the synthesis of these molecules comprise several evolutionarily distinct groups, of which class III is the largest. The domain structures of prokaryotic and eukaryotic class III NCs are diverse, including a variety of regulatory and transmembrane modules. Yet all members of this family contain one or two catalytic domains, characterized by an evolutionarily ancient topological motif (βααββαβ) that is preserved in several other enzymes that catalyze the nucleophilic attack of a 3′-hydroxyl upon a 5′ nucleotide phosphate. Two dyad-related catalytic domains compose one catalytic unit, with the catalytic sites formed at the domain interface. The catalytic domains of mononucleotidyl cyclases (MNCs) and diguanylate cyclases (DGCs) are called cyclase homology domains (CHDs) and GGDEF domains, respectively. Prokaryotic NCs usually contain only one catalytic domain and are catalytically active as intermolecular homodimers. The different modes of dimerization in class III NCs probably evolved concurrently with their mode of binding substrate. The catalytic mechanism of GGDEF domain homodimers is not completely understood, but they are expected to have a single active site with each subunit contributing equivalent determinants to bind one GTP molecule or half a c-diGMP molecule. CHD dimers have two potential dyad-related active sites, with both CHDs contributing determinants to each site. Homodimeric class III MNCs have two equivalent catalytic sites, although such enzymes may show half-of-sites reactivity. Eukaryotic class III MNCs often contain two divergent CHDs, with only one catalytically competent site. All CHDs appear to use a common catalytic mechanism, which requires the participation of two magnesium

S. C. Sinha (✉)
University of Texas Southwestern Medical Center at Dallas, Division of Infectious Diseases, Department of Internal Medicine,
5323 Harry Hines Blvd., Dallas, 75390-9113 TX, USA
e-mail: Sangita.Sinha@UTSouthwestern.edu · Tel.: +1-214-6487240 · Fax: +1-214-6480248

S. R. Sprang
University of Texas Southwestern Medical Center, Department of Biochemistry,
6001 Forest Park Rd., Dallas, 75390-8816 TX, USA

or manganese ions for binding polyphosphate groups and nucleophile activation. In contrast, mechanisms for purine recognition and specificity are more diverse. Class III NCs are subject to regulation by small molecule effectors, endogenous domains, or exogenous protein partners. Many of these regulators act by altering the interface of the catalytic domains and therefore the integrity of the catalytic site(s). This review focuses on both conserved and divergent mechanisms of class III NC function and regulation.

Introduction

Small-molecule second messengers such as inositol triphosphate, diacylglycerol, guanosine-5′-triphosphate-3′-diphosphate, Ca^{2+}, and the cyclic nucleotides (cNMPs), adenosine 3′-5′ cyclic monophosphate (cAMP), guanosine 3′-5′ cyclic monophosphate (cGMP) and bis-(3′-5′)-cyclic di-guanosine monophosphate (c-diGMP), are key components of intracellular signal transduction pathways in all cellular organisms. The first small-molecule second messenger to be identified was cAMP, while c-diGMP is the most recently discovered (Barzu and Danchin 1994; McCue et al. 2000; Romling et al. 2005). While cAMP has been found in most cellular organisms except plants, cGMP has been found chiefly in eukaryotes, and c-diGMP appears to be ubiquitous among prokaryotes (Cooper 2003; Linder and Schultz 2003; Romling et al. 2005; Shenoy and Visweswariah 2004). The cNMPs regulate cellular functions such as gene expression, metabolism, and ion flux in organisms ranging from prokaryotes to mammals (Romling et al. 2005; Taussig and Zimmermann 1998). In metazoans, cyclic nucleotides mediate processes such as cell growth, differentiation during embryogenesis, cardiac contractility, transmission of nerve impulses, learning and memory, and blood glucose homeostasis (Krupinski and Cali 1998; Smit and Iyengar 1998; Taussig and Zimmermann 1998), while in unicellular organisms they have been shown to regulate motility, chemotaxis, pathogenicity, response to osmotic stress and environmental acidification, cell-to-cell-communication, biofilm formation, and multicellular behavior (Kimura et al. 1997; Ladant and Ullmann 1999; Leppla 1982; Romling et al. 2005; Süsstrunk et al. 1998; Yahr et al. 1998). Intracellular levels of cNMPs are primarily regulated by their rate of synthesis, although localization or subcellular compartmentalization, as well as their rate of degradation by enzymes called phosphodiesterases, also plays an important role (Cooper 2003; Hanoune and Defer 2001). In vivo, cAMP, cGMP, and c-diGMP are synthesized by nucleotidyl cyclases (NCs): adenylyl cyclases (ACs), guanylyl cyclases (GCs), and diguanylate cyclases (DGCs), respectively. A comprehensive review by Barzu and Danchin grouped mononucleotidyl cyclases (MNCs) that had been identified into three classes on the basis of amino acid sequence, and summarized the biochemical information available for each class (Barzu and Danchin 1994). Subsequently, reviews of NCs have chiefly focused on the most universal of these three classes, the class III NCs. In the last few years, the structures of the catalytic domains of various class III NCs have been solved. This review will primarily focus on knowledge obtained from these structures in the context of available biochemical information.

Classification

All NCs that have been identified are grouped into five nonhomologous classes based on sequence similarity (Barzu and Danchin 1994; Cotta et al. 1998; Linder and Schultz 2003;

Sismeiro et al. 1998). Each of the five classes of cyclases is expected to have a different structural fold and mode of activity, suggesting that each class probably arose from different ancestral enzymes. Despite these key differences, all NCs use nucleoside triphosphates (NTPs) as substrate and catalyze identical chemical reactions, and consequently have convergently evolved some common features for binding and catalysis. Except for the class III NCs, enzymes belonging to the other classes appear to be MNCs that are strictly specific for ATP.

Class I NCs are ACs that have been only found in gram-negative, enteric, γ-proteobacteria such as *Escherichia, Yersinia*, *Haemophilus* and *Pseudomonas*. The class I ACs from these bacteria are approximately 850-amino-acid proteins that are thought to contain two domains: an N-terminal, catalytic domain of approximately 450 amino acids and a C-terminal, regulatory domain of approximately 500 amino acids (Barzu and Danchin 1994; Holland et al. 1988; Reddy et al. 1995a). The primary structure of all ACs that have been grouped in class I, which share between 50% and 99% sequence identity, is well conserved. The class I ACs were the first NCs to be identified, yet have not been extensively characterized and there are no representative structures. Therefore, residues important for the activity of these ACs have not yet been identified.

Class II NCs are AC exotoxins secreted by pathogenic prokaryotes such as *Bacillus anthracis, Bordetella pertussis*, and *Pseudomonas aeroginosa* (Barzu and Danchin 1994; Ladant and Ullmann 1999; Leppla 1982; Yahr et al. 1998). These ACs differ considerably in length, with the *B. anthracis, B. pertussis*, and *P. aeroginosa* enzymes comprising 800, 1,706, and 378 amino acids respectively. The catalytic fragments of each of these class II ACs are approximately 360 amino acids in length and share less than 30% sequence identity with each other. The architecture of the class II ACs from these three organisms diverges greatly, with the conserved catalytic fragment attached to a variety of domains thought to play a role in regulation. These cyclases are activated by different host cell factors and are inactive until they are injected into the host cell. Structures of the catalytic domains of two class II ACs, edema factor (EF) from *B. anthracis* and, more recently, CyaA from *B. pertussis*, have been determined (Drum et al. 2002; Guo et al. 2004, 2005; Shen et al. 2005).

Class III constitutes the largest and most diverse family of NCs. It includes all DGCs, GCs, and eukaryotic ACs identified to date, as well as ACs from many prokaryotes. The catalytic domains of class III NCs are approximately 180 amino acids in length. The catalytic domains of the class III MNCs, the ACs and GCs, are often called cyclase homology domains (CHDs), while those of the DGCs are called GGDEF domains, based on the presence of a highly conserved Gly-Gly-Asp-Glu-Phe sequence motif. Notably, the central Gly-Asp couple of this motif is a very highly conserved sequence feature of the CHDs as well. Both CHDs and GGDEF domains are highly divergent and therefore difficult to identify solely from sequence. In fact, only four residues, an aspartate, the Gly-Asp motif described above, and another glycine are well-conserved among all class III NCs (Fig. 1). The biochemical significance of the numerous variations among the catalytic domains of class III NCs, such as differences in residues implicated in catalysis and insertions in the core fold that may be responsible for varying modes of regulation, has yet to be completely understood.

The evolutionary relationship between CHDs and GGDEF domains has been previously investigated (Pei and Grishin 2001). It was noted that outliers among the GGDEF domains sometimes share higher sequence identity with some CHDs, than with other GGDEF domains. The small size of these domains combined with their divergent sequences prevented construction of a reliable phylogenetic tree, yet it was clear that GGDEF domains and CHDs belong to separate groups. GGDEF domains may be further subdivided into two clusters, one comprising of DGCs from eubacteria, and the other including DGCs from archaebacteria as

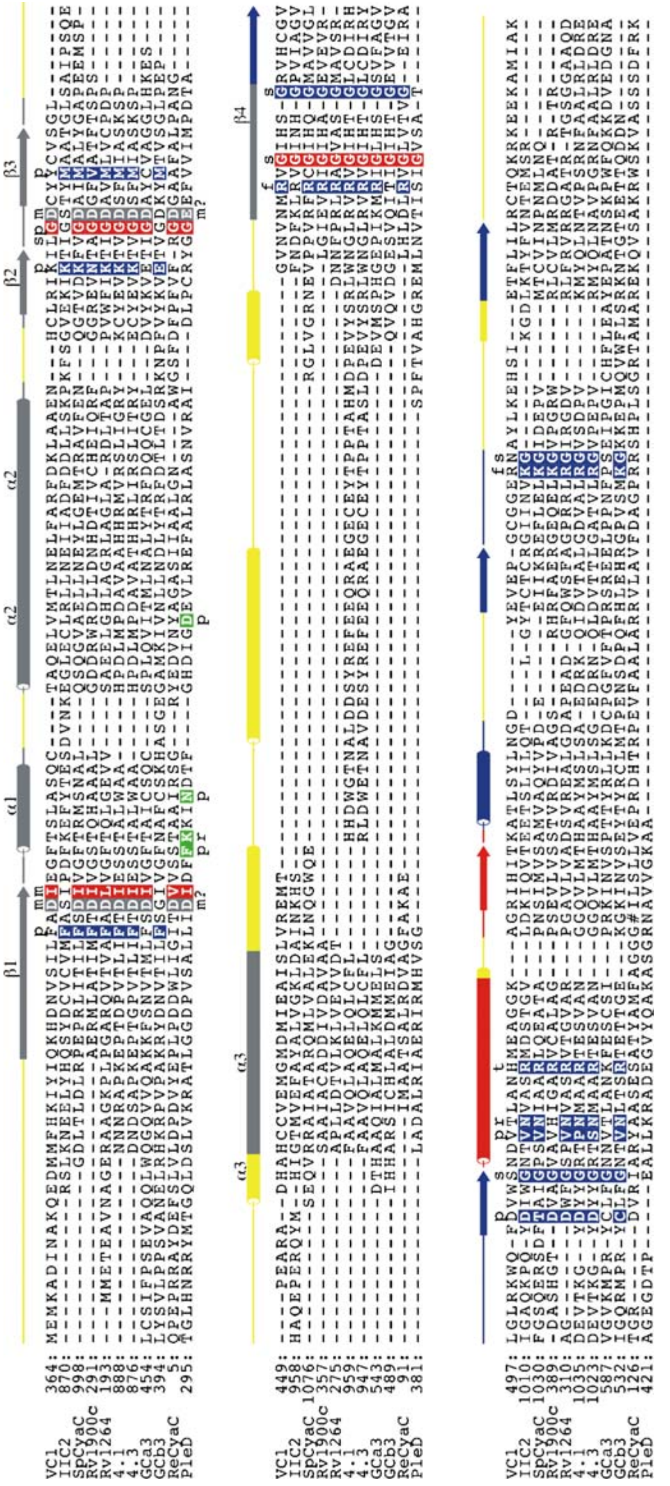
β1
α1
α2
α2
β2
β3
α3
α3
β4
VC1
IIC2
SpCyaC
Rv1900c
Rv1264
4.1
4.3
GCa3
GCb3
ReCyaC
PleD

◀ **Fig. 1** Structure-based sequence alignments of catalytic domains of class III NCs. Biological sources and either PDB codes for class III NCs of known structure or accession numbers for other class III NC sequences are: *VC1* Canine AC VC_1 (1CJK_A), *IIC2* Rat AC IIC_2 (1CJK_B), *SpCyaC Spirulina platensis* CyaC (1WC6), *Rv1900c* and *Rv1264 Mycobacterium tuberculosis* Rv1900c (1YBU) and Rv1264 (1Y11) respectively; *4.1* and *4.3 Trypanosoma brucei* GRESAGs 4.1 (1FX2) and 4.3 (1FX4) respectively, *GCa3* and *GCb3* Canine soluble GC1 subunits α3 (gi:65301169) and β3 (gi:65294809) respectively, *ReCyaC Rhizobium etli* CyaC (gi: 20530211), *PleD Caulobacter crescentus* (1W25). The first residue of each sequence in each alignment bloc is indicated. The "#" symbol indicates residues 151–191 of ReCyaC which are omitted from the alignment. Consensus secondary structure elements deduced from class III NCs of known structure are shown *above the alignment* and are numbered according to the core class III NC fold, and not in context of the individual full-length proteins. *Bold white letters* highlighted against *colored backgrounds* indicate conserved residues important for the activity of class III NCs. The role of these conserved residues is indicated *above* and *below* the alignment for CHDs and GGDEF domains, respectively, by: *s* structural, *m* metal-coordinating, *f* phosphate-bonding, *r* ribose-bonding, *p* purine-interacting. Secondary structure elements and conserved residues common to both class III NCs and type I DNA polymerases are highlighted in *gray*, those common to all class III NCs are highlighted in *red*, those conserved only among either the CHDs or GGDEF domains are highlighted in *blue* or *green*, respectively, and where possible, features unique to individual enzymes are shown in *yellow*. This figure was made using the program ALSCRIPT (Barton 1993)

well as some eubacteria. Recently, the first structure of a GGDEF domain, PleD, a DGC from *Caulobacter crescentus* was solved, and conclusively demonstrated that this domain belongs to the class III NCs (Table 1; Chan et al. 2004).

As for the GGDEF domains, some divergent CHDs share higher sequence identity with some GGDEF domains than with the more closely related members within the CHD family. Linder and Schultz have subdivided CHDs into subclasses IIIa–d based on variations in residues required for catalysis as well as the length of a β-ribbon located between a glycine and an aspartate that are conserved among most CHDs (Fig. 1; Linder and Schultz 2003). McCue et al. have subdivided mycobacterial CHDs into classes I–V according to the statistical occurrence of amino acids at each residue position (McCue et al. 2000). The functional, structural, and evolutionary implications of these subdivisions have yet to be completely explored. Available CHD structures include those of the C_1 domain of type V mammalian AC (VC_1) and the C_2 domain of type II mammalian AC (IIC_2), trypanosomal GRESAG 4.1 and 4.3, *Spirulina platensis* CyaC, and *Mycobacterium tuberculosis* Rv1900c, Rv1264, and Rv1625c (Table 1; Bieger and Essen 2001; Ketkar et al. 2006; Mou et al. 2005; Sinha et al. 2005; Steegborn et al. 2005a, b; Tesmer et al. 1997, 1999, 2000; Tews et al. 2005; Zhang et al. 1997).

The architecture of class III NCs diverges greatly. However, mammalian ACs, which have been the focus of extensive biochemical and structural analyses, are fairly well conserved. Nine of ten mammalian ACs that have been identified are membrane-bound AC (mAC) homologs sharing sequence identities ranging from approximately 50% to 90% (Sunahara et al. 1996) and are complex molecules consisting of two tandem repeats of a hexa-helical transmembrane domain and a cytoplasmic, catalytic CHD. Activity of these NCs requires intramolecular association between the N-terminal CHD (C_1) and C-terminal CHD (C_2) of each cyclase molecule (Dessauer and Gilman 1997; Dessauer et al. 1997; Whisnant et al. 1996; Yan et al. 1996). Studies of mACs have answered some of the basic questions about mechanisms of activity of this family. The function, regulation, and tissue distribution of different mammalian AC homologs have been summarized in several reviews (Cooper et al. 1994; Cooper 2003; Hanoune and Defer 2001; Krupinski and Cali 1998; Smit and Iyengar 1998; Sunahara et al. 1996; Sunahara and Taussig 2002; Tang et al. 1998; Taussig and Zimmermann 1998), and the structure and molecular basis of the catalytic mechanism and regulation of mammalian CHDs have been discussed (Hurley 1998, 1999; Simonds 1999; Tesmer and Sprang 1998). Prokaryotic class III NCs differ considerably in

Table 1 Structures of class III NCs. ATP analogs that have been co-crystallized with CHDs include 5′-(α-thio)-triphosphate (ATPαS), β-L-2′,3′-dideoxy-adenosine-5′-triphosphate (βLddATP) and α,β-methyleneadenosine 5′-triphosphate (AMPCPP). Pyrophosphate (PPi) and P-site inhibitors that have been co-crystallized with the mAC VC1-IIC2 heterodimer include 2′-deoxyadenosine 3′-monophosphate (2d3AMP) and 2′,5′-dideoxy-adenosine-3′-triphosphate (dd3ATP). 2′(3′)-*O*-(*N*-methylanthraniloyl)-guanosine-5′-triphosphate (MANT-GTP) is a nonphysiological inhibitor that binds to the active site of the mAC VC1-IIC2 heterodimer. Crystals for coordinate set 1WC6 contained bicarbonate; see text

PDB ID	Protein	Substrate/ product analogs	Metal A-site	Metal B-site	Regulatory molecules	Reference
Cyclase homology domains						
1AB8	IIC_2	–	–	–	Forskolin	Zhang et al. 1997
1AZS	VC_1-IIC_2	–	–	–	Forskolin, Gs_α	Tesmer et al. 1997
1CJK	VC_1-IIC_2	ATPαS	Mg^{2+}	Mn^{2+}	Forskolin, Gs_α	Tesmer et al. 1999
1CJU	VC_1-IIC_2	βLddATP	Mg^{2+}	Mg^{2+}	Forskolin, Gs_α	Tesmer et al. 1999
1CS4	VC_1-IIC_2	2d3AMP, PP_i	–	Mg^{2+}	Forskolin, Gs_α	Tesmer et al. 2000
1CUL	VC_1-IIC_2	dd3ATP, PP_i	Mg^{2+}	Mg^{2+}	Forskolin, Gs_α	Tesmer et al. 2000
1TL7	VC_1-IIC_2	–	Mn^{2+}	Mn^{2+}	MANTGTP	Mou et al. 2005
1YBT	Rv1900c	–	–	–	–	Sinha et al. 2005
1YBU	Rv1900c	AMPCPP	–	Mn^{2+}	–	Sinha et al. 2005
1Y10	Rv1264	–	–	–	–	Tews et al. 2005
1Y11	Rv1264	–	–	–	–	Tews et al. 2005
1YK9	Rv1625c	–	–	–	–	Ketkar et al. 2006
1FX2	GRESAG 4.1	–	–	–	–	Bieger and Essen 2001
1FX4	GRESAG 4.4	–	–	–	–	Bieger and Essen 2001
1WC0	CyaC	AMPCPP	–	Mg^{2+}	–	Steegborn et al. 2005b
1WC1	CyaC	ATPαS	Mg^{2+}	Mg^{2+}	–	Steegborn et al. 2005b
1WC6	CyaC	ATPαS	Mg^{2+}	Mg^{2+}	–	Steegborn et al. 2005b
1WC5	CyaC	AMPCPP	Displaced Mg^{2+}	Mg^{2+}	–	Steegborn et al. 2005b
2BW7	CyaC	AMPCPP	Displaced Mg^{2+}	Mg^{2+}	Catechol	Steegborn et al. 2005a
GGDEF domains						
1W25	PleD	c-diGMP	–	–	c-diGMP	Chan et al. 2004

length, as their catalytic domains may be linked to a wide variety of other domains responsible for sensing appropriate signals and regulation or interaction with other proteins. In contrast to the mammalian ACs, class III MNCs from lower organisms often have a simpler organization than the mammalian ACs, and typically contain only one CHD.

ACs in the bacteria *Aeromonas hydrophila* and *Prevotella ruminicola* were identified on the basis of their ability to complement *Escherichia coli* cyclase knockout mutants (Cotta et al. 1998; Sismeiro et al. 1998). These ACs do not share detectable sequence similarity with the three classes of NCs described above, or to each other, nor do they appear to contain, in appropriate register, residues that have been shown to be important for function in the class II and class III cyclases. Thus, they have been placed in classes IV and V, respectively (Cotta et al. 1998; Linder and Schultz 2003; Sismeiro et al. 1998). Very recently, the structure of a class IV AC from *Vibrio parahaemolyticus* and *Yersinia pestis* has been solved (Gallagher et al. 2006). Yet another AC—CyaC from *Rhizobium etli*, also identified by its ability to restore AC activity in *E. coli* cyclase knockout mutants—has been proposed to constitute a sixth class of cyclases (Tellez-Sosa et al. 2002). However, several key residues required for binding and catalysis by the class III NCs are present at similar relative positions in this protein, although it shares less than 15% sequence identity with other class III NCs that have been studied (Fig. 1). Thus, in the absence of further structural, mutational, or biochemical evidence, it is likely that this enzyme and other close homologs may simply constitute yet another subfamily of class III NCs.

Structural homology of class III NCs

The first NC structures determined were those of class III CHDs belonging to the mammalian ACs. The core fold of the CHDs was determined from the structure of the mammalian IIC_2 domain (Zhang et al. 1997) and verified by subsequent structures of CHDs (Table 1; Fig. 2a). The core fold of the GGDEF domains was determined more recently from the *Caulobacter crescentus* PleD structure (Fig. 2b; Chan et al. 2004). As has been previously discussed, numerous proteins, including the palm domain of type I DNA polymerases and the catalytic domains of class III NCs share a ferredoxin-like βαββαβ structural motif, such that the αββ connection between the two βαβ repeat units is left-handed (Fig. 2c; Artymiuk et al. 1997; Murzin 1998; Pei and Grishin 2001). This motif corresponds to β1-α2-β2-β3-α3-β4 of the class III NC core fold, in which the strands form a part of the central β-sheet (β2-β3-β1-β4). In all class III NCs and the palm domain of type I DNA polymerases, a short helix, α1, is inserted between β1 and α2, and the α2 helix is long. Thus, these two protein families have a common core βααββαβ structural motif (Fig. 2a–c).

Two aspartic acid residues that are invariant among CHDs have been shown to be critical for catalysis. These residues are located on the core βααββαβ structural motif; the first is the penultimate residue of β1, while the second is located at the C-terminus of the β2-β3 loop (Figs. 1 and 3a). These two aspartates are also very highly conserved in the GGDEF domains, although in many homologs the β2-β3 loop aspartate, which corresponds to the central residue of the GGDEF motif, is substituted by a glutamate (Figs. 1 and 3b). The core βααββαβ structural motif of the type I DNA polymerases also bears two invariant aspartates critical for catalysis at topologically equivalent positions (Fig. 3c). The conservation of the βααββαβ structural motif (Fig. 2), combined with the preservation of catalytically important residues (Fig. 3) in class III NCs and type I DNA polymerases, suggests that these two enzyme families share a common ancestor.

The core βααββαβ structural motif of class III NCs is further extended by a helix (α4) and another strand (β5) (Figs. 1 and 2a–b). Thus, as was previously predicted, the CHDs and GGDEF domains have a common order of core secondary structure elements consisting of β1-α1-α2-β2-β3-α3-β4-α4-β5, that folds into a compact α/β sandwich (Pei and Grishin

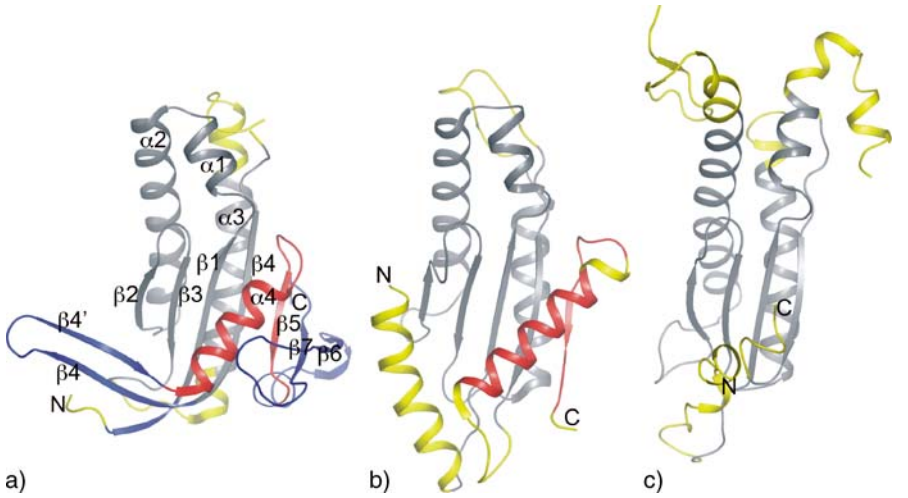

Fig. 2a–c The βααββαβαβ structural motif conserved in class III NCs and DNA polymerases. Secondary structure elements are colored and labeled as in Fig. 1. This and all molecular figures were made using the program PYMOL (http://pymol.sourceforge.net/). **a** CHD fold with secondary structural elements labeled. **b** GGDEF domain fold. **c** Palm domain of DNA polymerase

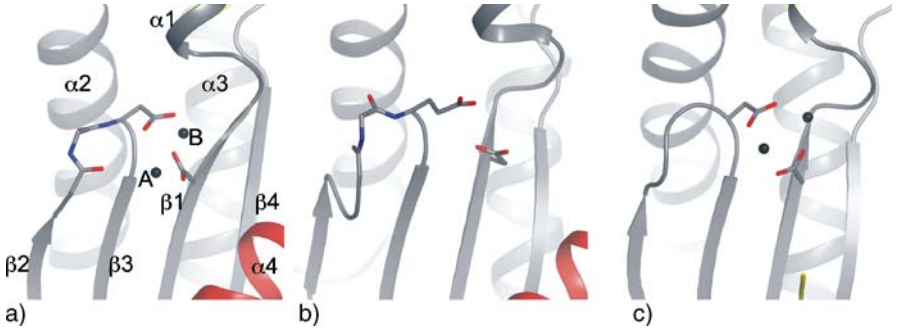

Fig. 3a–c Structural equivalence residues highly conserved in class III NCs and DNA polymerases. Secondary structure elements are colored and labeled as in Fig. 1. Conserved residues—including the two acidic residues conserved in both these enzyme families, and the β2-β3 loop glycine conserved in class III NCs—are shown in molecular detail. Metal ions are indicated by *black spheres*. **a** CHD. **b** GGDEF domain. **c** Palm domain of type I DNA polymerase

2001). This catalytic core fold is conserved among all class III NCs and consists of a central, five-stranded, antiparallel β-sheet of strand order β2-β3-β1-β4-β5, with three helices, α1–α3, on the back face of this sheet and another helix, α4, on the front face (Figs. 1 and 2a–b). In addition to the two invariant acidic residues on β1 and the β2-β3 loop, two conserved glycines are located at structurally equivalent positions in all class III NCs (Figs. 1 and 3a–b). The first glycine precedes the conserved acidic residue on the β2-β3 loop. Thus, the β2-β3 loop of all class III NCs bears a conserved Gly-Asp pair, which in DGCs corresponds to the second residue of the GGDEF motif. The Φ,Ψ dihedral angles of this glycine map to unfavorable regions of the Ramachandran plot in all available class III NC structures, indicating that a glycine at this position may be important for maintaining a specific conformation of the β2-β3 loop. The second glycine conserved in class III NCs maps to the middle of β4 and is sometimes substituted by other small residues such as alanine. This

glycine is conserved due to steric constraints arising from the packing of α4 against β4 (Pei and Grishin 2001). This β4 glycine is not conserved in the palm domains of type I DNA polymerases, as the core βααββαβ structural motif of these domains is not extended by the α4-β5 extension present in class III NCs.

Distinct insertions into the conserved class III NC core fold further distinguish the CHDs from the GGDEF domains. The GGDEF domain of *C. crescentus* PleD is modified by a subdomain composed of a β-hairpin (β0-β0′) and a helix (α0) that precedes the class III NC core fold as well as by another β-hairpin (β3′-β3″) inserted between β3 and α3 of the class III NC core (Fig. 2b). The function and conservation of these insertions among the GGDEF domains remains to be fully investigated. However, sequence alignments suggest that the β3′-β3″ is absent among archaeal and some bacterial GGDEF domains and may be a distinguishing feature between subgroups of GGDEF domains (Pei and Grishin 2001).

The class III NC core fold in all CHDs is modified by two insertions, which constitute the most variable features of CHDs (Figs. 1, 2a, and 4). The first of these insertions, named the dimerization arm, is introduced between β4 and α4, and consists of a β-ribbon comprising C-terminal residues of the extended β4 strand and an antiparallel β-strand (β4′). The dimerization arm is bounded by two almost-invariant glycines (Fig. 1). The first of these glycines corresponds to the last β4 residue within the class III NC core, while the second, which is occasionally substituted by a serine, precedes α4 of the class III NC core at the end of the dimerization arm (Fig. 1). The Φ,Ψ dihedral angles for both these glycines map to unfavorable regions of the Ramachandran plot in all available CHD structures, indicating that glycines at these position facilitate the bending of β4 and the tight turn between the dimerization arm and α4. The length of this dimerization arm defined by these two invariant glycines ranges from 10 to 19 residues and constitutes an important distinguishing feature among the four CHD subclasses designated by Linder and Schultz (Figs. 1 and 4; Linder and Schultz 2003). In some homologs, the N-terminal residues of β1 are also hydrogen-bonded to the β-ribbon of the dimerization arm, forming a three-stranded β-sheet of strand order β1-β4-β4′ (Fig. 2a). The second CHD-specific insertion follows β5 of the class III NC core fold and consists of a helix, α5, followed by an antiparallel β-hairpin, β6-β7 (called β7-β8 in structures of CHDs) that extends the central β-sheet by two strands. Compared to other CHD structures, β5 is shorter in mammalian VC_1 domains, and the β6-β7 hairpin is replaced by an Ω loop consisting of two short α-helices (Tesmer et al. 1997). A glycine, whose Φ,Ψ dihedral angles also map to generously allowed regions of the Ramachandran plot, is almost invariant on the β6-β7 loop of all CHDs in which the following residue is a basic residue that hydrogen-bonds the polyphosphate group of substrate or product, suggesting that this glycine assists in positioning the basic residue in these CHDs (Fig. 1).

According to the Linder and Schultz classification, the mammalian VC_1 and IIC_2 domains and the Rv1625c CHD belong to class IIIa, *S. platensis* CyaC belongs to class IIIb, *M. tuberculosis* Rv1900c and Rv1264 belong to class IIIc, and the trypanosomal GRESAG ACs belong to class IIId (Linder and Schultz 2003). Thus, structures of CHDs from nearly the full spectrum of class III NCs have now been determined (Fig. 4 and Table 1). All of these CHDs have the same CHD core fold, but have diverged with respect to insertions such as the length of the β4-β4′ ribbon (dimerization arm), the length and structure of the α5-β6-β7 subdomain, and the presence of variable insertions such as the δ-subdomain of the trypanosomal GRESAG proteins (Fig. 4).

Fig. 4 CHDs from subclasses IIIa–d. Structural elements constituting the core class III NC fold are much better conserved than the CHD-specific features. PDB IDs of the superimposed CHDs from subclasses a–d are CanineVC_1 (1CJK_A) in *green*, *S. platensis* CyaC (1WC6) in *blue*, *M. tuberculosis* Rv1900c (1YBU) in *black*, and Trypanosomal GRESAG 4.1 (1FX2) in *red*, respectively

Quaternary structure of class III NCs

Structures of the catalytically competent VC_1-IIC_2 heterodimers in complex with substrate analogs or inhibitors (Tesmer et al. 1997) conclusively demonstrated that CHDs are active only as dimers, as had been suggested on the basis of solution studies of these domains (Dessauer and Gilman 1997; Dessauer et al. 1997; Scholich et al. 1997a; Tang and Gilman 1995; Whisnant et al. 1996; Yan et al. 1996). The GGDEF domains have not been studied as extensively, but the recent structure of *C. crescentus* PleD, in complex with the c-diGMP, suggests that dimerization is a prerequisite for catalysis by these enzymes as well (Chan et al. 2004).

The mammalian ACs were the first NCs to be extensively studied. Structures of catalytically competent VC_1-IIC_2 heterodimers demonstrated that CHDs form intramolecular, isologous dimers (Tesmer et al. 1997). As the two CHDs are homologous, but have non-identical sequences and associated structural variations, these intramolecular heterodimers are pseudo-symmetrical. Class III NCs from lower organisms typically contain only one CHD and are active as intermolecular homodimers (Guo et al. 2001; Linder and Schultz 2003). Structures of three homodimeric NCs, two from *M. tuberculosis* and one from the cyanobacterium *S. platensis*, indicate that these homodimeric CHDs may form either pseudo-symmetrical or perfectly symmetrical, isologous homodimers, depending on structural differences between the chemically identical CHDs (Sinha et al. 2005; Steegborn et al. 2005b; Tews et al. 2005). Thus, packing interactions between dyad-related CHDs may be symmetrical or pseudo-symmetrical.

Dimerization contacts between CHDs are extensive, burying 1,500–3,500 Å of the total accessible surface area at the dimer interface and involving both hydrophobic and electro-

static interactions. One face of the dimer, termed the ventral face (the side of the dimer from which substrates can enter the catalytic site), bears a shallow trough that runs along the dimer interface perpendicular to the dyad axis (Fig. 5a). The β2-β3 hairpins from each subunit abut each other at the center of the dimer interface, dividing this trough into two nucleotide-binding sites related by the dyad axis. While the two β2-β3 hairpins always form the inner edge of each site, the outer edge is usually bordered by the dimerization arm of one CHD packed against α2, the α1-α2 turn and in some structures, β2 of the other CHD. Additionally, the β4′-α4 turn of one subunit contacts the α1-α2 turn of the other subunit (Fig. 5a). In some CHDs dimerization may be significantly perturbed by mutations on the dimerization arm or the β2-β3 hairpin (Ketkar et al. 2004, 2006; Shenoy et al. 2003). There are significant variations in these packing interactions, not only between dimers of different CHDs, but also between the dyad-related elements of pseudo-symmetrical dimers. Notably, compared to the class IIIa and class IIIb CHDs, the dimerization arms of the class IIIc CHDs are shorter (Fig. 1; Linder and Schultz 2003) and make fewer inter-domain contacts, accounting for a decrease of approximately 1,500 Å of surface area buried at the dimer interface of these CHDs (Sinha et al. 2005; Tews et al. 2005).

Each of the two dyad-related sites at the CHD dimer interface constitutes a potential active site (Fig. 5a). Residues from each domain line both potential active sites. The β2-β3 hairpin of each CHD, which participates in both sites, divides each CHD into two structural modules. The first module comprises the β1-α1-α2-β2-β3-α3-β4 core structural motif that is conserved among class III NCs and type I DNA polymerases and provides most of the determinants for binding divalent metal cations and polyphosphate groups, as well as elements essential for chemical reactions involving a 3′-5′-phosphodiester bond. The second module is composed of the α4-β5 core fold extension present in all the class III NCs, as well as the two CHD-specific insertions, the β4-β4′ dimerization arm and the α5-β6-β7 extension (Fig. 2a) and provides most of the elements for binding the nucleotide base and ribose. Within each CHD, the first module contributes residues to one binding site, while residues from the second module participate in the dyad-related binding site.

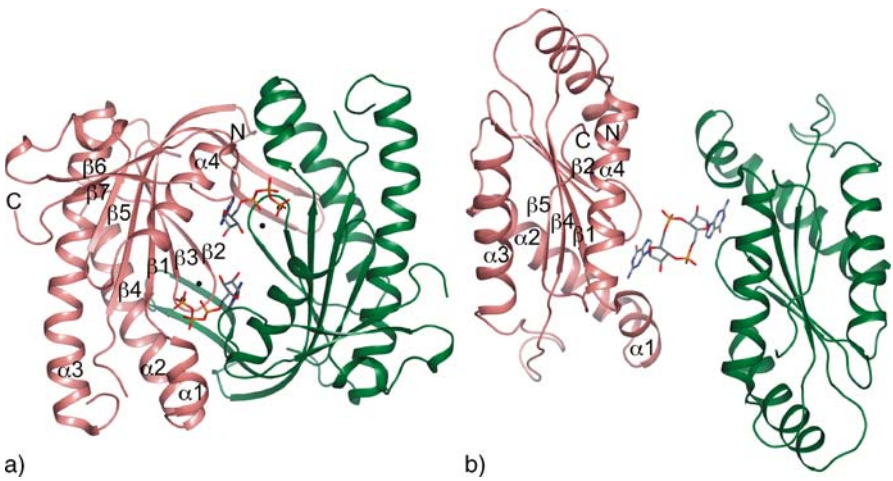

Fig. 5 Dimers of class III NCs. The two subunits are colored *green* and *salmon*, and active sites are indicated by bound ligands depicted in molecular detail. Secondary structure elements and termini of the polypeptide chain of one subunit are labeled as in Fig. 1. **a** CHD domain catalytic dimer. **b** Proposed GGDEF domain catalytic dimer. Note the different dyad axes relating the subunits of each of these dimers

Oligomerization of GGDEF domains in their active state in solution has not been clearly established. However, the *C. crescentus* PleD structure in complex with the product c-diGMP indicates that a single GGDEF domain provides binding determinants for only one GTP, or half of a c-diGMP molecule, suggesting that dimerization is essential for activity (Chan et al. 2004). Indeed, the binding determinants for the other half of the c-diGMP molecule are provided by a second PleD molecule, related to the first by the dyad axis of the c-diGMP (Fig. 5b). However, it is not certain whether the dimers observed in crystals correspond to a biologically relevant arrangement of subunits as, unlike most physiological dimers, the two subunits do not make any direct protein–protein interaction and are linked only by the shared c-diGMP molecule (Fig. 5b). The paucity of interactions between subunits is also in contrast to the extensive dimerization contacts seen between subunits in the CHD dimers. Although, like the CHD homodimers, the active site of GGDEF domains is also located at the dimer interface, unlike the CHD homodimers, each GGDEF domain contributes all the elements to bind one GTP molecule (Fig. 5). Further, unlike the CHD homodimers, which have two chemically equivalent active sites, the GTP-binding sites of two GGDEF domains combine to form a single active site (Fig. 5). The proposed two-fold symmetry axis that relates subunits in a catalytically competent GGDEF domain dimer is different from that which relates subunits in a CHD dimer.

Active sites and catalytic mechanism

NCs catalyze the synthesis of 3′,5′ cNMPs from their respective NTPs. Most NCs are specific for either ATP or GTP. The cyclization reaction has been observed to proceed with an inversion of stereochemistry in the class III mammalian ACs, suggesting that it involves the in-line nucleophilic attack of the ATP 3′-hydroxyl on the 5′ α-phosphate, leading to a pentavalent-phosphate transition state intermediate. and subsequently to the products cAMP and pyrophosphate (Eckstein et al. 1981). It is likely that this chemical reaction mechanism is common to all class III NCs. Thus, all class III NC active sites are constrained by the common objectives of binding NTP, distinguishing between ATP and GTP, increasing the nucleophilicity of the 3′-hydroxyl, as well as a mechanism that facilitates the release of products. Further, as the cyclization reaction catalyzed by the MNCs is intramolecular, the active sites of these enzymes are expected to have the ability to stabilize the strained transition state ribose conformation, required for the displacement of the 5′ pyrophosphate by the 3′-hydroxyl (Tesmer et al. 2000). In the next two sections we discuss and compare the mechanism of binding, catalysis, and substrate release by CHDs and GGDEF domains. In all subsequent descriptions of NC active sites, functionally important or conserved residues are identified by the secondary structure elements on which they are located.

CHD active sites

Structures of the catalytically competent VC_1-IIC_2 heterodimers, and subsequently of CHD homodimers, demonstrated that, in both hetero- and homodimers the active site is located in a deep groove at the interface of the CHDs (Sinha et al. 2005; Steegborn et al. 2005b; Tesmer et al. 1997; Tews et al. 2005). Structures of the mammalian VC_1-IIC_2 CHD heterodimers as well as the *M. tuberculosis* Rv1900c and the *S. platensis* CyaC CHD homodimers, in complex with various ligands (Table 1) have enabled investigators to elucidate the general mode by which CHDs bind the substrate ATP (Fig. 6a). NC active sites require elements to bind

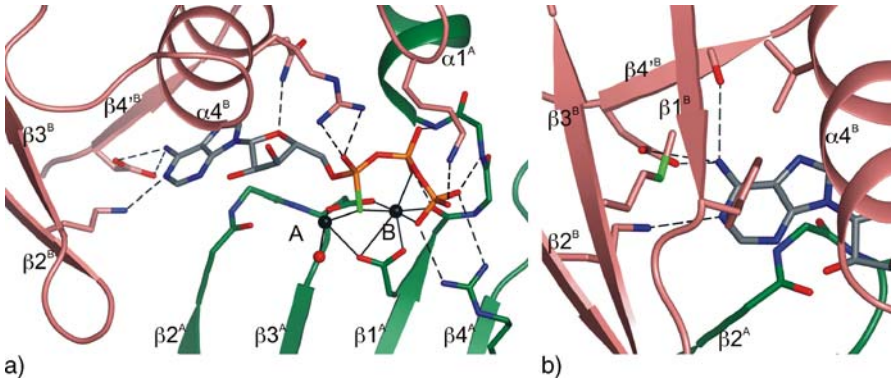

Fig. 6a, b Active site of class III MNCs. The two CHDs are colored as in Fig. 5 and secondary structures labeled as in Fig. 1. Secondary structures from the module comprising the core βααββαβ structural motif of one CHD are denoted by a *superscripted A* (^{A}), while those from the second module comprised of class III NC-specific or CHD-specific elements from the other CHD are denoted by a *superscripted B* (^{B}). Molecular details of bound ligands and of protein residues that play a role in substrate binding and catalysis are shown. *Solid, black lines* represent the coordination sphere of the bound metals while *dashed, black lines* indicate hydrogen bonds. **a** ATP analog ATPαS-bound active site. Protein elements that obstruct this view of the active site are not shown. **b** Purine-binding sub-site

the negatively charged polyphosphate group and stabilize the ribose and purine moieties of the NTP. In CHDs the former role is primarily performed by electrostatic interactions with basic amino acids and coordination by divalent metal cations, which in turn are coordinated by carboxylate and carbonyl groups from the protein. In contrast, the mechanism of binding the ribose and purine appear to be less specific and therefore less well conserved, chiefly involving hydrophobic packing and stacking interactions, although polar interactions play an important role in purine recognition. As described above, residues from each CHD contribute to both dyad-related binding sites (Sinha et al. 2005; Steegborn et al. 2005b; Tesmer et al. 1997). Thus, each dyad-related site is formed by residues from the β2-β3 loop of both CHDs, residues from the first module comprising the core βααββαβ structural motif of one CHD denoted by a superscripted A (^{A}), and residues from the second module made up of class III NC-specific or CHD-specific elements from the other CHD, denoted by a superscripted B (^{B}) (Fig. 6a).

Coordination of metal in CHD active sites

Like most other enzymes that catalyze reactions involving phosphodiester bonds, such as RNA and DNA polymerases and ribozymes, CHDs require divalent metal cations for catalysis (Beese and Steitz 1991; Doublié and Ellenberger 1998; Steitz 1993, 1999; Steitz et al. 1994; Steitz and Steitz 1993; Tesmer et al. 1997; Zimmermann et al. 1998). Based on evidence from mutagenesis (Zimmermann et al. 1998), and crystal structures of the VC_1-IIC_2 heterodimer in complex with ATP analogs R_p-ATPαS or βLddATP (Tesmer et al. 1999), the active site binds two divalent metal cations (Fig. 6a). These metal cations occupy sites referred to as "A" and "B," in analogy to corresponding sites in DNA and RNA polymerases (Doublié and Ellenberger 1998; Tesmer et al. 1999). The B-site is typically occupied by Mg^{2+} or Mn^{2+} in structures of CHDs to which NTPs (or pyrophosphate) are bound, indicating that binding of metal at this site is a prerequisite to binding the β and γ phosphates of the substrate ATP, or the by-product of ATP cyclization, pyrophosphate (Mou et al. 2005; Sinha et al. 2005; Steegborn et al. 2005b; Tesmer et al. 1999). The B-site metal cation is typically

bound in an octahedral coordination shell that includes at least one (but sometimes both) carboxylate from each of $\beta1^A$ Asp^A and $\beta2^A$-$\beta3^A$ loop Asp^A, the first backbone carbonyl of the $\beta1^A$-$\alpha1^A$ loop (often called the phosphate-binding or P-loop^A), two or three oxygens from the polyphosphate moiety, and one or more water molecules (Fig. 6a). The A-site metal is usually tetrahedrally coordinated by either one or both carboxylate oxygens from $\beta1^A$ Asp^A and $\beta2^A$-$\beta3^A$ Asp^A, one or two oxygens from the ATP α-phosphate, and a water molecule (Tesmer et al. 1999). In the structure of *S. platensis* CyaC in complex with ATPαS, the A-site metal is also hydrogen-bonded to the 3′-hydroxyl of R_p-ATPαS, consistent with its proposed role in catalysis (see below; Steegborn et al. 2005b). In the crystal structures of several CHD complexes, the A-site appears to be occupied by a water molecule, or only partially occupied by metal ion (Sinha et al. 2005; Steegborn et al. 2005b; Tesmer et al. 1999). The A-site may be sterically blocked in structures of VC_1:IIC_2 bound to P-site inhibitors with 3′ phosphate substituents (Tesmer et al. 1997, 2000). Although Mg^{2+} is thought to be the physiologically relevant cofactor for most CHDs, bonds constituting the coordination shell of each metal site are longer than those typical for Mg^{2+}. This may explain the enhanced activity of most CHDs in the presence of larger divalent metal cations like Mn^{2+}. Further, structural evidence indicates that the A-site preferentially binds and is inhibited by Zn^{2+}, perhaps because a tetrahedral coordination geometry is inherently favored at this site, while the B-site preferentially binds metal cations that favor an octahedral coordination geometry such as Mn^{2+}, Ca^{2+}, Sr^{2+}, and Eu^{2+} (Steegborn et al. 2005b; Tesmer et al. 1999). The two aspartates responsible for coordinating metal, $\beta1^A$ Asp^A and $\beta2^A$-$\beta3^A$ loop Asp^A, are invariant among most CHDs and constitute the best-conserved features of CHD active sites. This emphasizes the importance of metal cations, not only in binding ATP, but also for catalysis. The importance of these aspartates, and implicitly the metals they coordinate, is underscored by evidence that mutations of these residues dramatically reduce activity (Liu et al. 1997; Sinha et al. 2005; Tang et al. 1995; Tesmer et al. 1999). The two metal sites are separated by 3.9 Å in most enzymes that utilize two divalent metal cations to catalyze chemical reactions involving phosphodiester bonds (Beese and Steitz 1991; Doublié and Ellenberger 1998; Steitz 1993, 1999; Steitz and Steitz 1993). Consistent with this, the two sites are separated by 3.5–4.5 Å in most structures of the VC_1-IIC_2 heterodimer in complex with various ligands, as well as that of *M. tuberculosis* Rv1900c CHDs in complex with AMPCPP, where the A-site is occupied by water (Sinha et al. 2005; Tesmer et al. 1999, 2000). However, considerable variation in the placement and ligation of Mg^{2+} is observed in the structures of CHDs in complex with certain nonphysiological inhibitors, such as that of VC_1:IIC_2 bound to MANT-GTP (Mou et al. 2005), and of *S. platensis* CyaC in complex with AMPCPP (Steegborn et al. 2005b).

Phosphate binding in CHD active sites

Binding of phosphate groups in CHD active sites is quite variable and a variety of ligands, including nucleotide 5′ monophosphates, nucleotide 3′ monophosphates, nucleotide 3′ triphosphates, and pyrophosphate, can be accommodated (Table 1). Polyphosphate moieties of substrate analogs and the product pyrophosphate are bound to essentially the same subsite of the CHD active site. This subsite is located at the C-terminal edge of the central sheet ($\beta2^A$-$\beta3^A$-$\beta1^A$-$\beta4^A$) of the conserved βααββαβ structural motif (Fig. 6a). The conformation of the polyphosphate groups bound in this subsite, as well as details of interactions with protein groups, varies substantially among different ligand complexes, although some general features are preserved. In general, the polyphosphate group binds such that the α- and β-phosphates are extended over the $\beta2^A$-$\beta3^A$ loop and the γ-phosphate is stabilized over

a positively charged pocket formed by the three-residue P-loop^A ($\beta1^A$-$\alpha1^A$ loop) and the helix dipole of $\alpha1^A$ (Fig. 6a). The phosphate groups are stabilized via coordination by metal, as well as by hydrogen bonds to various positively charged protein groups such as the amides of the P-loop^A and conserved basic side-chains.

As mentioned in "Coordination of metal in CHD active sites," binding of metal at the B-site is a prerequisite for binding polyphosphate. The B-site metal usually coordinates and stabilizes both β- and γ-phosphates and often the α-phosphate as well. In contrast, the A-site metal most often coordinates the α-phosphate, and only occasionally either the ribose-α phosphate bridging oxygen or the β-phosphate. Backbone groups of the three-residue P-loop^A, are involved in binding the polyphosphate. The characteristic conformation of this loop is stabilized by hydrophobic packing interactions of the last β1 residue, which is usually a conserved isoleucine (Fig. 1). The main chain carbonyl of the last β1 residue and main chain amides of the first and second residues of the P-loop hydrogen-bond, either one or both, the β- and γ-phosphates. Three highly conserved basic residues—$\beta4^A$ Arg^A, $\alpha4^B$ Arg^B, and $\beta6^B$-$\beta7^B$ Lys^B—also play key roles in stabilizing the polyphosphate (Figs. 1 and 6a). The $\beta4^A$ Arg^A appears poised to form bidentate salt bridges with the γ-phosphate, but is located just beyond optimal hydrogen-bonding distance in most structures of CHD dimers in complex with ligands that contain polyphosphate. The $\beta6^B$-$\beta7^B$ Lys^B usually ion pairs with the γ-phosphate, or sometimes with either the α- or β-phosphate. Mutation of either of these residues usually increases K_m, consistent with their role in binding substrate (Dessauer et al. 1997; Sinha et al. 2005; Tang et al. 1995). The $\alpha4^B$ Arg^B often hydrogen-bonds the α-phosphate or occasionally the α-β bridging oxygen and has been proposed to stabilize the pentavalent α-phosphate transition state intermediate (Sinha et al. 2005; Tesmer et al. 1999). Consistent with this role, mutating this residue usually shows the rate of reaction, but does not impact affinity for substrate (Sinha et al. 2005; Tang et al. 1995; Yan et al. 1997b).

In structures of *S. platensis* CyaC in complex with substrate analogs, a conserved asparagine from $\alpha4^B$ hydrogen-bonds the oxygen bridging either the ribose and α-phosphate, or the α- and β-phosphates (Steegborn et al. 2005b). However, this may be a unique feature of *S. platensis* CyaC, as equivalents of this $\alpha4^B$ Asn^B do not make equivalent contacts in the mammalian VC_1-IIC_2 heterodimers or Rv1900c CHD homodimers. Finally, in addition to these conserved contacts, the polyphosphate group in different protein complexes has been observed to form additional interactions, which include water-mediated hydrogen bonds to different protein groups, as well as direct hydrogen bonds to nonconserved residues.

Binding of ribose in CHD active sites

The ribose ring is bound in the space between the $\beta2^A$-$\beta3^A$ loop and $\alpha4^B$ (Fig. 6a). Like the pyrophosphate moiety, the conformation of the ribose ring varies, and both 2′- and 3′-endo conformations have been observed. Further, in the structures of VC_1-IIC_2 in complex with βLddATP, the ribose ring is inverted relative to the orientation seen in complexes of CHDs with ligands such as R_p-ATPαS or AMPCPP, as well as P-site inhibitors (Tesmer et al. 1999). However, in contrast to the polyphosphate, the ribose ring makes few direct contacts with the protein, and these are conserved poorly among CHDs (Figs. 1 and 6a). The 2′ and 3′-hydroxyls usually do not directly contact any protein groups, but each may be involved in one to three, nonconserved, water-mediated bonds. However, in structures of *S. platensis* CyaC in complex with two Mg^{2+} and AMPCPP or R_p-ATPαS, the 3′-hydroxyl is hydrogen-bonded to the $\alpha4^B$ Arg^B or the A-site metal, respectively (Steegborn et al. 2005b). While the mechanistic relevance of the former is unclear, the latter is clearly pro-catalytic as discussed later in the context of the catalytic mechanism. The ribose ring oxygen is hydrogen-bonded

to amide of the $\alpha 4^B$ Asn^B in structures of the mammalian VC_1-IIC_2 heterodimers in complex with R_p-ATPαS, and is implicated in orienting the substrate or transition state (or both) for catalysis (Tesmer et al. 1999). This conclusion is supported by mutations of the mammalian enzymes (Yan et al. 1997b). In *M. tuberculosis* Rv1900c CHDs, $\alpha 4^B$ Asn^B is substituted by a histidine, which does not participate in direct interactions with ATP. Mutational evidence further confirms that this residue is not required for catalysis by Rv1900c CHDs (Sinha et al. 2005). Structures of *S. platensis* CyaC indicate that in these enzymes, the $\alpha 4^B$ Asn^B is present in a location topologically equivalent to that in the mammalian VC_1-IIC_2 heterodimers, but is not located within hydrogen-bonding distance of the ribose oxygen of the bound NTP. It is possible that further closure of the active site is required to allow formation of this hydrogen bond or, as in Rv1900c, this residue does not play a role in catalysis. As equivalents of $\alpha 4^B$ Asn^B are variously substituted or missing in many CHDs identified from genome sequences, it is likely that either the specific elements for stabilizing the ribose ring and orienting substrate are not general prerequisites of the CHD active site or that these elements vary greatly among the CHDs.

Base recognition by CHD active sites

Selection of correct nucleotide substrates by NCs is essential to the fidelity of cyclic nucleotide-mediated signal transduction. In contrast to the ribose and phosphate, the purine ring is inflexible and it appears to form identical interactions in different nucleotide complexes with the same enzyme. However, there is substantial variation in the mechanism of purine recognition used by different CHDs. In all CHDs, the purine base binds in a hydrophobic pocket formed by conserved residues from the $\beta 2^B$-$\beta 3^B$ hairpin, $\beta 1^B$, $\beta 2^B$, $\alpha 4^B$, and the dimerization arm^B(Figs. 1 and 6b). The hydrophobic packing interactions include edge-to-face stacking with a conserved aromatic residue from $\beta 1^A$ that precedes the invariant $\beta 1^A$ Asp^A by two residues (Figs. 1 and 6b). In addition to these interactions, the purine ring is stabilized by stacking against either one of the two peptide planes that involve the $\beta 2^A$-$\beta 3^A$ loop glycine that is invariant in all class III NCs (Figs. 1 and 6b). There are few polar interactions with the purine ring, and these serve chiefly to discriminate between ATP and GTP (Figs. 1 and 6b). Due to the nonspecific nature and variability of many of these interactions, it has been difficult to completely understand the mechanism of base recognition by CHDs. Variations in the modes by which CHDs accomplish this function have been summarized in a recent review (Linder 2005). In this section, we outline general features but describe only results of structure-based studies in some detail.

Typically, ACs are highly specific for ATP with no detectable activity with GTP (Coudart-Cavalli et al. 1997; Guo et al. 2001; Kasahara et al. 2001; Linder et al. 2002, 2004; Shenoy et al. 2005; Sunahara et al. 1998; Weber et al. 2004), although Cya1, an AC from *Rhizobium meliloti* has detectable GC activity (Beuve et al. 1993). In comparison, various GCs have been shown to have significant AC activity also (Beuve 1999; Linder et al. 1999, 2000; Sunahara et al. 1998; Tucker et al. 1998). Two residues conserved among AC CHDs—the $\beta 2^B$-$\beta 3^B$ hairpin Lys^B, which precedes the invariant β2-β3 loop Gly-Asp by two residues, and the dimerization arm^B Asp^B—were identified as key determinants of base specificity from structures of the mammalian VC_1-IIC_2 heterodimers (Figs. 1 and 6b; Tesmer et al. 1997). These two residues hydrogen-bond the N1 and N6 of the ATP adenine and preclude binding of GTP. Recent structures demonstrate that in *S. platensis* CyaC, ATP is similarly selected by hydrogen bonds between the topologically equivalent residues, a $\beta 2^B$-$\beta 3^B$ hairpin Lys^B and a dimerization arm^B Thr^B and the N1 and N6 of the ATP adenine (Steegborn et al. 2005b). In the mammalian ACs, a third residue—a

dimerization arm^{A} Gln^{A}—that in VC_1 precedes the equivalent of IIC_2 dimerization arm^{B} Asp^{B} by two residues (Fig. 1) and is within the van der Waals contact radius of the $\beta2^{B}$-$\beta3^{B}$ hairpin Lys^{B}, has been proposed to play a role in substrate selection (Sunahara et al. 1998). Structures of GCs are not yet available, but the sequence equivalents of $\beta2^{B}$-$\beta3^{B}$ hairpin Lys^{B} and dimerization arm^{B} Asp^{B} of the mammalian ACs are conserved among GCs (Fig. 1) as a glutamate and cysteine, respectively, and are proposed to hydrogen-bond the N2 and O6 of guanine (Fig. 1; Beuve 1999; Sunahara et al. 1998; Tucker et al. 1998). A GC arginine, which is the equivalent of the VC_1 dimerization arm^{A} Gln^{A}, is proposed to orient the conserved glutamate by salt bridges as well as packing interactions. However, mutational analyses suggest that these residues may not be the sole determinants of base specificity in these enzymes. Mutating the mammalian IIC_2 $\beta2^{B}$-$\beta3^{B}$ hairpin Lys^{B}, the dimerization arm^{B} Asp^{B}, and the dimerization arm^{A} Gln^{A} to glutamate, cysteine, and arginine, respectively, does not switch specificity of the VC_1-IIC_2 heterodimer, but rather converts it into a nonspecific NC with reduced activity (Sunahara et al. 1998). Mutations of the $\beta2^{B}$-$\beta3^{B}$ hairpin Lys^{B} and the dimerization arm^{B} Asp^{B} in ACs from lower organisms often abolish all enzyme activity (Kasahara et al. 2001; Ketkar et al. 2006; Shenoy et al. 2003, 2005; Sunahara et al. 1998). In contrast to ACs, mutation of the glutamate, cysteine, and arginine found in GCs to a lysine, aspartate, and glutamine, respectively, converted GCs to a stringently ATP-specific AC (Beuve 1999; Linder et al. 2000; Sunahara et al. 1998; Tucker et al. 1998). In fact, the single conversion of cysteine to an aspartate was adequate for switching specificity, suggesting that the dimerization arm^{B} Asp^{B} is the most important determinant for substrate specificity while the other residues play supporting roles.

The recently characterized mycobacterial nucleotidyl cyclase Rv1900c can use both ATP and GTP as substrate, with a 14-fold preference for ATP (Sinha et al. 2005). Apart from Rv1900c, only one other prokaryotic enzyme has been shown to have GC activity (Ochoa de Alda et al. 2000). Strikingly, in Rv1900c the mammalian IIC_2 $\beta2^{B}$-$\beta3^{B}$ hairpin Lys^{B} that hydrogen-bonds the adenine N1 is replaced by an asparagine and may account for its reduced specificity, with the dimerization arm^{B} Asp^{B} establishing the preference for ATP. However, structures of Rv1900c in complex with AMPCPP indicated that neither the $\beta2^{B}$-$\beta3^{B}$ loop Asn^{B}, nor the dimerization arm^{B} Asp^{B} hydrogen-bond the adenine N1 or N6, and therefore are probably not the main determinants for the preferential use of ATP as substrate. Instead of hydrogen-bonding to the adenine, the $\beta2^{B}$-$\beta3^{B}$ loop Asn appears to sterically enforce binding of the purine ring in a half-of-sites binding mechanism discussed in "Evolution of Class III NC active sites." Correspondingly, the mutation of $\beta2^{B}$-$\beta3^{B}$ loop Asn^{B} does not significantly impact substrate specificity or enzyme activity, although inexplicably the dimerization arm^{B} Asp^{B} mutants have higher affinity for both ATP and GTP. The preference for ATP in Rv1900c has been attributed to nonlocalized general determinants such as electrostatic gradients from helix dipoles or peptide planes, shape complementarity, and size of the active site (Sinha et al. 2005). Additionally, interactions with backbone groups, such as the hydrogen bond between the adenine N6 and the carbonyl of the residue following the dimerization arm^{B} Asp^{B} observed in structures of VC_1-IIC_2 heterodimers may further select for ATP, and against GTP (Tesmer et al. 1997, 1999). It is likely that such general determinants play a role in purine specificity in all CHDs. In ACs, such general determinants probably dictate the preference for ATP, while the $\beta2^{B}$-$\beta3^{B}$ hairpin Lys^{B}–dimerization arm^{B} Asp^{B} couple enforce the strict specificity for ATP. In contrast, general determinants in the active site of GCs appear to allow binding of both ATP and GTP, with the preference for GTP dictated chiefly by the glutamate-cysteine couple.

Catalysis by CHDs

Although the structures of CHDs in complex with various ligands tell us much about binding the substrate ATP, none of these structures completely mimics the binding of the putative transition state. The product cAMP, which is rapidly released, may be the best analog. The transition state intermediate is expected to have a 3′-endo ribose conformation that positions the 3′-hydroxyl for in-line displacement of the pyrophosphate, with a pentavalent α-phosphate, whose negative charge is stabilized by the $\beta4^B$ Arg^B. As in many DNA polymerases, ribozymes, and phosphatases that employ a mechanism of two-metal ion catalysis, the A-site metal is expected to play an indispensable role in catalysis by CHDs. As the 3′-hydroxyl is a weak nucleophile, it has been proposed that metal bound at the A-site increases the nucleophilicity of the ATP 3′-hydroxyl (Tesmer and Sprang 1998). Indeed, consistent with the predicted role of the A-site metal as a Lewis acid, in structures of *S. platensis* CyaC in complex with two Mg^{2+} and R_p-ATPαS, the ribose 3′-hydroxyl is hydrogen-bonded to the A-site metal (Steegborn et al. 2005b). However, it is unlikely that this structure completely mimics the transition state, as the 3′-hydroxyl is not positioned for an in-line attack on the α-phosphate. In contrast to the nearly invariant orientation of the purine ring in substrate analogs bound to CHDs, the conformational flexibility of the ribose and pyrophosphate groups—both between different enzymes as well as between different structures of the same enzyme—may be indicative of the flexibility required to attain the strained transition state intermediate. Consequently, the variability captured in different crystal structures may represent an inherent feature of CHD active sites.

Product binding and release by CHDs

There are no structures of CHDs in complex with the products cAMP and pyrophosphate, perhaps because the same mechanism that enables release of products in the normal course of catalysis prevents the product-bound state from being captured in a crystal structure. In the mammalian ACs, cAMP appears to be released first, and the release of the pyrophosphate appears to be the rate-limiting step (Dessauer and Gilman 1997; Dessauer et al. 1999). This may be true for all CHDs. P-site inhibitors that, in the presence of pyrophosphate, are uncompetitive—dead-end inhibitors of the mammalian ACs—have been shown to bind to the VC_1-IIC_2 heterodimer active site, suggesting that these complexes may mimic binding of the products in the active sites (Tesmer et al. 2000). The binding sites of these inhibitors are very similar to that described above for the substrate analogs. However, as the P-site inhibitors do not significantly inhibit most homodimeric ACs, it is possible that complexes with mAC CHDs may not accurately represent the product-bound state in all CHDs. There may be subtle variations in the mode of binding—and consequently release—of products by different CHDs. For example, based on a superposition of cAMP on P-site inhibitors bound in the active site of the VC_1-IIC_2 heterodimer, it was proposed that steric clashes between the cyclized phosphate moiety and the A-site metal as well as the $\beta2^B$-$\beta3^B$ loop Asn^B resulted in the preferential release of cAMP (Tesmer et al. 2000). However, a similar steric restriction is not observed when cAMP is superimposed on the AMPCPP-bound structure of Rv1900c (Sinha et al. 2005). It is possible that catalysis proceeds only upon formation of a more closed conformation than observed in this structure of Rv1900c, which might then lead to a steric clash similar to that proposed for the mammalian ACs. Alternately, it is possible that the $\beta2^B$-$\beta3^B$ loop Asn^B that appears to regulate binding of the purine ring in Rv1900c, also regulates the release of the product cAMP by a similar mechanism.

Binding and catalysis by GGDEF domains

The structure of PleD, a DGC from *C. crescentus*, in complex with the product c-diGMP provides clues to the active site of the GGDEF domains (Chan et al. 2004). Like the CHDs, the GGDEF domain active site is located at the C-termini of the strands constituting the core βααββαβ motif. Further, like the CHDs, dimerization appears to be a prerequisite for catalysis. However, there appears to be no further similarity in the mode by which CHDs and GGDEF domains bind nucleotide. While in the CHDs, dimerization is required to bind a single NTP or cNMP, dimerization of the GGDEF domains is required because a single GGDEF domain appears to provide all of the determinants to bind only one GTP or half of a c-diGMP molecule while a second GGDEF domain, related to the first by the twofold symmetry axis of the c-diGMP, provides the determinants to bind the other GTP or the other half of the c-diGMP molecule (Fig. 5b and 7).

There are no metals bound in the structure of the c-diGMP-bound PleD complex, yet the two invariant aspartates that coordinate metal in the CHDs, the β1 Asp and β2-β3 loop Asp, are conserved at equivalent structural locations in GGDEF domains as an aspartate, and either an aspartate or a glutamate, respectively (Fig. 2a–b). However, the orientation of each guanine nucleotide moiety of diGMP in the catalytic site of PleD is the reverse of that of ATP analogs bound to CHDs, such that the ribose phosphate moiety is extended over the β2-β3 loop but directed away from the β1 strand (Fig. 7). In this orientation, the α-phosphate is hydrogen-bonded to the backbone amide of the second glycine of the GGDEF motif, which maps to the β2-β3 loop. The ribose ring is stabilized by hydrogen bonds between the ribose 2′-hydroxyl and the amide of a conserved α1 asparagine, as well as between the ribose 3′-hydroxyl and the amino group of a conserved lysine, which is the second residue of α1. The guanine ring is placed over a hydrophobic patch formed by side chains from α1 and α2 and is stabilized by edge-to-face stacking interactions with a conserved phenylalanine that is the first residue of α1 (Figs. 1 and 7). Hydrogen bonds involving the guanine N3/N2 and N1 with a conserved α1 Asn and α2 Asp, respectively, provide specificity for GTP over ATP.

Given the conservation of residues involved in key contacts with the guanine ring of c-diGMP, it is likely that the guanine ring from the substrate GTP also occupies a similar

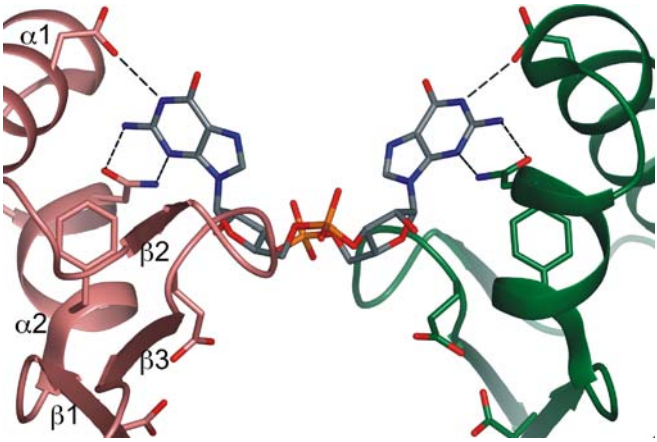

Fig. 7 Proposed active site of class III DGCs. The two GGDEF domains are colored as in Fig. 5 and secondary structures labeled as in Fig. 1. Molecular details of bound ligands and of protein residues that play a role in substrate binding and catalysis are shown. *Dashed, black lines* indicate hydrogen bonds

position and makes the same contacts. However, the position of the ribose and phosphate groups is likely to be flexible. Based on the c-diGMP-bound PleD structure, Chan et al. suggest that the mechanism of base recognition by the GGDEF domain sterically precludes binding of the GTP γ-phosphate over the β1-α1 loop, which constitutes the P-loop of CHDs. Instead, they predict that the β- and γ-phosphates of GTP are probably accommodated close to the first glycine of the GGDEF motif on the β2-β3 loop while a Mg^{2+} ion is coordinated by carboxylates from the glutamate constituting the fourth residue of this motif. Such a binding mode for GTP would preclude involvement of a second metal ion coordinated by the β1 aspartate and the β2-β3 loop glutamate/aspartate, which are conserved in both CHDs and GGDEF domains, as this metal would be too distant from the ribose 3′-hydroxyl or pyrophosphate group to play any role in binding or catalysis. Thus, the proposed mechanism employs only a single metal ion bound at a site distinct from the A- and B-metal sites of CHD dimers. Chan et al. further suggest that the central acidic residue of the GGDEF motif may act as a general base to deprotonate the GTP 3′-hydroxyl, priming it for attack on the 5′-phosphate of another GTP molecule. Dimers of GTP-bound GGDEF domains would orient the activated GTP molecules such that the 3′-hydroxyl of one is poised to attack the 5′-phosphate of the other. In this scheme, the amino group of the conserved α1 Lys would serve to stabilize the pentavalent phosphoryl transition state, as well as the pyrophosphate leaving group. This mechanism of catalysis does not define the role of the conserved β1 Asp that is invariant among GGDEF domains, CHDs, and DNA polymerases. Thus, although the c-diGMP-bound PleD structure has provided valuable insights into the structure and mode of product binding by GGDEF domains, structures of GGDEF domains in complex with substrate analogs and metal ions will be crucial to defining the mode of binding substrate and the mechanism of catalysis employed by DGCs.

Evolution of class III NC active sites

It is highly probable that CHDs, GGDEF domains, and palm domains of type I DNA polymerases all evolved from a common ancestor. These domains not only share a common core βααββαβ structural motif (Fig. 2), but also two invariant acidic residues located at topologically equivalent positions on this motif, the C-terminus of β1 and the β2-β3 loop (Fig. 3). Further, these two invariant acidic residues, and the βααββαβ core structural motif, also constitute the sequence and structural features, respectively, conserved best within each type of domain (Figs. 1 and 4).

In type I DNA polymerases and CHDs, the two invariant aspartates coordinate two divalent metal cations (Tesmer and Sprang 1998; Tesmer et al. 1999). These metal cations appear to have at least three distinct roles. The first is to bind and stabilize the negative charge on the NTP polyphosphate that contains the 5′-phosphate linked by the phosphodiester bond. Metals at both A- and B-sites appear to be involved in this function. The second role, involving only the A-site metal, is to increase the nucleophilicity of the 3′-hydroxyl. And the third role, involving chiefly the B-site metal, is to stabilize the leaving pyrophosphate group. All three of these functions appear to be well-conserved among both CHDs and DNA polymerases. Thus, the core βααββαβ structural motif appears to have evolved from a more ancient, and possibly more promiscuous, motif bearing two invariant acidic residues optimally positioned to coordinate two metals to bind NTP polyphosphates and to catalyze the formation of 3′-5′-phosphodiester bonds. The role of the equivalent acidic residues of GGDEF domains and any metals they may coordinate remains to be verified. In the GGDEF domains, an additional glutamate, corresponding to the fourth residue of the GGDEF mo-

tif, is conserved at the N-terminus of β3 and has been postulated to coordinate metal at a site distinct from either the A- or B-metal sites (Chan et al. 2004). Interestingly, although not present in the CHDs, a glutamate is also highly conserved at an equivalent location in the type I DNA polymerases, which, like the GGDEF domains, catalyze the formation of intermolecular 3′-5′-phosphodiester bonds.

Glycines on the β2-β3 loop and β4 are invariant in almost all class III NCs, indicating that these residues arose early in the evolution of these NCs, probably concurrently with the class III NC fold. The absence of a side-chain at the invariant β2-β3 loop glycine position prevents occlusion of purine-binding subsite in the CHDs, and probably part of the nucleotide-binding site in GGDEF domains as well. Additionally, in CHDs, the Φ and Ψ dihedral angles of this glycine map to unfavorable regions of the Ramachandran plot, facilitating a specific conformation of the β2-β3 loop and allowing one of the peptide planes of this glycine to stabilize the ATP purine ring by stacking interactions. Thus, this glycine plays a direct role in binding substrate in CHDs. The β4 glycine facilitates packing of α4 against β4, thereby positioning β4 relative to the βααββαβ motif. In CHDs, α4 contributes important residues to the active sites of these MNCs.

Although the βααββαβ structural motif and the two invariant acidic residues constitute a conserved module used to bind polyphosphate groups and catalyze the formation of 3′-5′-phosphodiester bonds by the class III MNCs and DGCs as well as the type I DNA polymerases, each enzyme family has evolved markedly different elements to bind and recognize the purine and ribose groups of the substrate NTPs. In type I DNA polymerases, the elements that interact with the nucleotide base and ribose are chiefly provided by the fingers domain, which is inserted between α1 and α2 of the βααββαβ structural motif. The fingers domains are typically much more divergent than the βααββαβ structural motif-containing palm domain of these enzymes (Brautigam and Steitz 1998). In CHDs, elements from the second structural module, comprising the class III NC and CHD-specific insertions, are responsible for several of the key interactions with the nucleotide base and ribose. However, in contrast to DNA-polymerases and CHDs, the c-diGMP bound PleD structure suggests that in GGDEF domains elements of the βααββαβ structural motif may also be responsible for binding purine and ribose.

While DNA polymerases function as monomers to catalyze the formation of 3′-5′-phosphodiester bonds, the class III NCs appear to be active only as dimers. However, the GGDEF domains and CHDs are expected to have markedly different modes of dimerization. Two GGDEF domains are expected to associate to form a homodimer with a single, interfacial, catalytically competent active site. The two subunits of a GGDEF domain dimer are expected to be related by the dyad symmetry of the bound substrates or products, with each subunit providing identical determinants to bind a single GTP molecule or half a c-diGMP molecule. In contrast, two CHDs associate to form two potential active sites at the dimer interface. As discussed in section “CHD active sites”, each of these potential active sites is lined by elements from two structural modules, the first module comprising the βααββαβ structural motif of one subunit and the second module comprising the class III NC and CHD-specific insertions of the other subunit. In CHDs, therefore, elements of the second structural module—especially the CHD-specific insertions, the mode of dimerization, and of binding NTPs—all probably evolved concurrently from a more primitive βααββαβ structural motif.

CHDs from lower organisms appear to function as homodimers with two chemically identical, interfacial active sites related by the dimer dyad axis. In most of these CHD homodimers the two dyad-related active sites are also structurally and mechanistically equivalent and symmetrical (Fig. 8a; Steegborn et al. 2005b). Unexpectedly, however, although the Rv1900c CHDs form homodimers with chemically equivalent, dyad-related active sites,

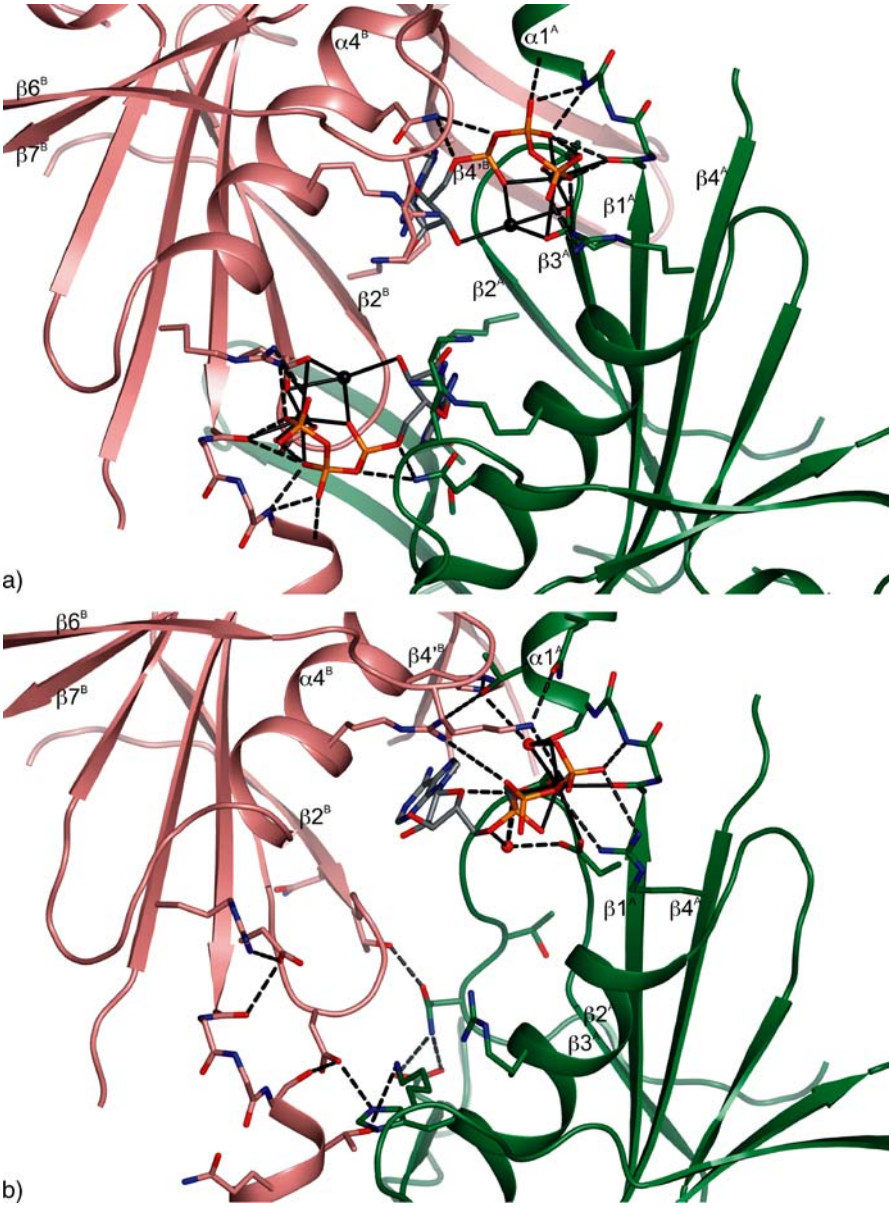
β6B
β7B
α4B
α1A
β4'B
β1A
β4A
β3A
β2B
β2A
a)
β6B
β7B
α4B
β4'B
α1A
β2B
β1A
β4A
β2A
β3A
b)

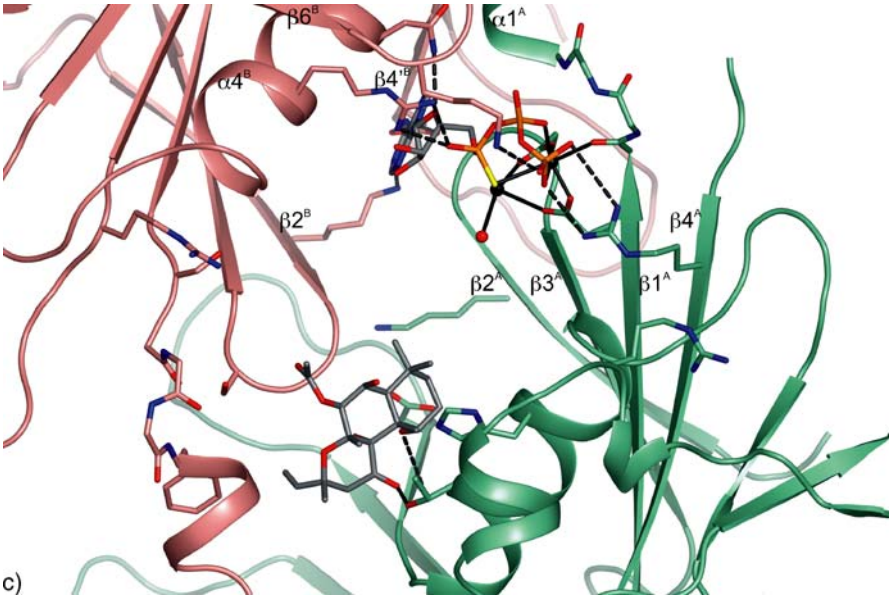

Fig. 8a–c Dyad-related sites of CHD dimers. Subunits, molecular details, bonds, and labels are depicted as in Fig. 6. **a** The two symmetrical, dyad-related active sites of the *S. platensis* CyaC CHD homodimer. Both sites are occupied by ATPαS. **b** The two chemically equivalent, yet structurally and mechanistically asymmetrical, dyad-related active sites of the Rv1900c CHD homodimer. Only one active site is occupied by AMPCPP. **c** The two asymmetrical, dyad-related binding sites of the VC_1-IIC_2 heterodimer include a single functional active site occupied by ATPαS and a nonfunctional site occupied by forskolin

these sites are structurally asymmetrical (Fig. 8b; Sinha et al. 2005). This asymmetry, which is amplified in the AMPCPP-bound, catalytically competent state, appears to be a consequence of the β2-β3 hairpin that participates simultaneously in both active sites of the dimer. As discussed earlier, this hairpin bears a conserved polar-X-X-G-D motif, of which the first residue participates in one active site, while the last two residues contribute to the dyad-related active site. The first residue of this motif interacts with the purine base, the glycine is important for structure and also for stabilizing the bound purine ring, and the aspartate is essential for binding metal and polyphosphate, and for catalysis. While the first polar residue of this motif is an adenine-specifying lysine or guanine-specifying glutamate in ACs and GCs, respectively, in Rv1900c it is an asparagine. Instead of hydrogen-bonding to the purine ring, this asparagine from one CHD points away from the AMPCPP-bound site, while in the other it appears to partially obstruct the ATP purine-binding subsite, preventing ATP from binding in this site (Fig. 8b; Sinha et al. 2005). Thus, although Rv1900c is catalytically active as a homodimer, the two active sites of the homodimer appear incapable of simultaneously binding ATP and catalyzing the synthesis of cAMP, suggesting a mechanism of half-of-sites reactivity. Mutational and biochemical data provide further support for a mechanism of half-of-sites reactivity (Sinha et al. 2005). Finally, while the two potential active sites in homodimeric ACs are chemically identical, those of the pseudo-symmetrical CHD heterodimers are not. Thus, in contrast to the homodimeric ACs, usually only one of the two potential active sites of the pseudo-symmetrical mammalian CHD heterodimers has the full complement of residues required for catalysis (Fig. 8c; Tesmer et al. 1997). The mechanism of half-of-sites reactivity observed for homodimeric Rv1900c may provide clues to the mechanistic variability that may have preceded and facilitated the evolution of the more

complex, asymmetrical, intramolecular heterodimers from the simpler, intermolecular homodimers. This chemical, structural, or mechanistic asymmetry of CHD dimers provides a unique mechanism of regulating NC activity.

Regulation of class III NCs

The mechanism of substrate binding and catalysis is fairly well conserved within the CHDs, and probably within the GGDEF domain subfamily as well. However, the stimuli that affect the synthesis of cNMPs, as well as the modes by which activity of class III MNCs or DGCs are regulated, vary greatly. Implicit in this divergent regulation is the presence of diverse regulatory domains that allow different signals to be transduced to either the CHDs or GGDEF domains, and expressed in varying levels of NC activity.

The regulation of mammalian ACs has been the subject of intense investigation, which has been summarized in several reviews (Cooper et al. 1994; Cooper 2003; Hanoune and Defer 2001; Krupinski and Cali 1998; Smit and Iyengar 1998; Sunahara et al. 1996; Sunahara and Taussig 2002; Tang et al. 1998; Taussig and Zimmermann 1998). However, much remains to be understood about the molecular mechanism by which these enzymes are regulated. As mentioned in section on "Classification", ten ACs have been identified in mammals. Mammalian ACs have a fairly uniform architecture. The CHDs of all ten mammalian ACs function as intramolecular heterodimers. Nine of these ACs are mACs, while the tenth is a "soluble" AC (sAC) (Buck et al. 1999). There are several striking differences between the mACs and sAC. The nine mACs are homologs consisting of two consecutive repeats of a hexa-helical transmembrane domain and a cytoplasmic CHD. The sAC gene contains two tandem cytoplasmic CHDs linked to a "AAA" nucleotide binding domain (NBD) followed by a segment of approximately 800 residues that is uncharacterized in structure and function and the sAC appears to be active as various C-terminally truncated forms (Buck et al. 1999; Feng et al. 2005; Geng et al. 2005; Jaiswal and Conti 2001; Roelofs and Van Haastert 2002).

The role of the two hexa-helical transmembrane domains, M_1 and M_2, of the mACs is not well understood. It is likely that as a membrane anchor for the CHDs, the transmembrane domains not only serve to localize the cytoplasmic, catalytic CHDs to membrane surfaces but also are essential for targeting to the plasma membrane, where they are in close proximity to various effector molecules that regulate the mACs. Further, it is likely that these domains play key roles in AC oligomerization. Experiments using various combinations of truncated, duplicated, inverted, chimeric, or fully swapped membrane anchors from different mAC homologs indicated that the M_1 and M_2 domains also form intramolecular heterodimers and that type-specific association is critical for enzyme activity (Seebacher et al. 2001). These type-specific interactions may be important mechanisms for preventing inappropriate cross-isoform interactions. Further, the M_2 domains may also be involved in intermolecular homodimerization, which may be indicative of mechanisms of inhibition involving the formation of catalytically incompetent CHD homodimers (Gu et al. 2002). It has also been suggested that the transmembrane domains may enable mACs to specifically associate with other membrane proteins, and these interactions balanced against homo-oligomerization properties of mACs may play an important role in regulation of catalytic activity. Thus, different types of mACs may localize to separate membrane rafts along with the specific integral-transmembrane proteins or membrane-anchored proteins that regulate them, creating local microdomains of finely tuned cAMP levels within a single cell (Cooper 2003, 2005; Noyama and Maekawa 2003; Zehmer and Hazel 2003). Finally, some

studies suggest that the transmembrane domains may also serve as direct sensors of membrane capacitance and potential, or membrane lipid and fluidity composition and regulate CHD activity in response to these stimuli (Cooper et al. 1998; Reddy et al. 1995b).

The mACs are differentially regulated by numerous effectors including the G proteins that transduce the numerous signals sensed by G protein-coupled receptors; Ca^{2+}, that regulates ACs either directly or indirectly via calmodulin; kinases such as calmodulin kinase protein kinase C and protein kinase A; and phosphatases such as calcineurin (Cooper et al. 1994, 1995; Cooper 2003; Hanoune and Defer 2001; Krupinski and Cali 1998; Mons et al. 1998; Smit and Iyengar 1998; Sunahara et al. 1996; Sunahara and Taussig 2002; Tang et al. 1998; Taussig and Zimmermann 1998). Unlike the mACs, the sAC does not appear to be regulated by any of these macromolecular effectors, but instead appears to be directly regulated by small molecules such as Ca^{2+}, bicarbonate, and catechols (Cann et al. 2003; Chen et al. 2000; Geng et al. 2005; Hyne and Garbers 1979; Jaiswal and Conti 2003; Litvin et al. 2003). The role of the NBDs and the transmembrane domain in these ACs is not yet understood.

Compared to higher eukaryotes, signaling pathways that regulate MNCs in prokaryotes and lower eukaryotes are simpler and more direct. Indeed, most CHDs from these lower organisms are linked in *cis* to one or more of a large variety of sensory/regulatory domains that are thought to directly transduce signals to the CHDs. Homologs of many of these domains have been shown to play similar regulatory roles in other signal transduction pathways. These domains include:

- Small molecule-binding domains such as GAF (an abbreviation derived from domains in cGMP-binding diesterases, adenylyl cyclases, and the *E. coli* transcription factor, FhlA); PAS (domains in period clock protein, Aryl hydrocarbon receptor, single-minded protein); and BLUF (flavin-containing, PAS domain like blue-light receptor) domains. Domains with diverse functions such as HAMP (domains in histidine kinases, adenylyl cyclases, methyl-accepting chemotaxis proteins and phosphatases) domains; ATPase domains; histidine kinase domains; RAS-associated domains; two-iron, two-sulfur cluster containing domains; leucine-rich repeats; TPR (tetratricopeptide repeat) domains; helix-turn-helix DNA binding domains; single helical transmembrane anchors; hexa-helical transmembrane domains. A few domains whose fold and function have not yet been identified (Linder 2005; Shenoy and Visweswariah 2004).

In addition, CHDs from lower organisms may be directly regulated by small molecules such as bicarbonate and Ca^{2+} (Cann et al. 2003; Chen et al. 2000; Masuda and Ono 2005; Steegborn et al. 2005b). Little is known about the molecular mechanism by which these diverse regulators influence CHD activity, although recent studies have begun to investigate the structural basis of these mechanisms.

Structures of the mammalian VC_1-IIC_2 heterodimer in complex with the cAMP synthesis-stimulating Gα subunit ($G\alpha_s$) greatly enhanced our understanding of how the mACs are regulated by macromolecular effectors (Tesmer et al. 1997, 1999, 2000). The most extensive interaction between $G\alpha_s$ and the VC_1-IIC_2 heterodimer involves the insertion of the $G\alpha_s$ switch II helix into a groove between the $\alpha1^B$-$\alpha2^B$ and $\alpha3^B$-$\beta4^B$ loops of IIC_2 (Fig. 9a). As $G\alpha_s$ can bind to IIC_2 monomers and disrupt IIC_2 homodimers in the absence of VC_1, it is likely that this interaction provides most of the binding energy required for the formation the AC-$G\alpha_s$ complex and simultaneously prevents formation of nonproductive C_2 homodimers. Although homodimerization of C_1 or C_2 domains would be irrelevant to regulation in vivo for monomeric mAC molecules, it could be a significant

mechanism of regulation if mACs assemble as dimers or oligomers (Gu 2002). In addition to the switch II-mediated interaction, the α3-β5 loop of $G\alpha_s$ interacts with the N-terminus of VC_1, which packs against the CHD dimerization arm^A (Tesmer et al. 1997). Although this interaction is not essential for binding of $G\alpha_s$ to mACs, it is essential for the upregulation of catalytic activity by $G\alpha_s$ (Sunahara et al. 1997). This interaction may promote the formation of a more closed conformation of the intramolecular C_1-C_2 heterodimers essential for activity. Indeed, binding of potent substrate analogs, such as ATPαS, is accompanied by movement of C_1 toward the C_2 domain, thereby aligning the P-loop^A of C_1 with the purine-binding elements in β4′^{B} and α4^B of C_2, and closing the catalytic site (Fig. 9b; Tesmer et al. 1999). This transition may be abetted by the binding of $G\alpha_s$. Finally, mutation data suggest that other regions of $G\alpha_s$, such as the α4-β6 loop, may be involved in additional interactions, presumably with AC regions not included in the VC_1 and IIC_2 constructs used for the crystal studies (Scholich et al. 1997b; Sunahara et al. 1997; Yan et al. 1997a). Thus, $G\alpha_s$ functions as an allosteric activator of mammalian ACs by facilitating both the relative rearrangement of the C_1 and C_2 domains to form catalytically competent heterodimers, as well as by stabilizing catalytically competent conformations of loops and residues involved in catalysis.

$G\alpha_s$-mediated stimulation of type I, V, and VI mACs is opposed by the inhibitory Gα subunit, $G\alpha_i$ (Chen et al. 1997; Taussig et al. 1993). Myristoylation of the $G\alpha_i$ subunit is required for this inhibitory activity. $G\alpha_i$ does not compete for the AC binding site of the $G\alpha_s$ subunit; rather, the inhibitory and stimulatory Gα subunits appear to bind to distinct sites on mACs (Taussig et al. 1994; Wittpoth et al. 1999). Evidence that $G\alpha_i$ and VC_1 form a 1:1 complex, combined with mutational analysis, suggest that switch II, and perhaps the α4-β6 loop of $G\alpha_i$, are involved in the interaction with VC_1, while the α1^A-α2^A and α3^A-β4^A loops of VC_1 play key roles in binding of $G\alpha_i$ (Dessauer et al. 1998; Wittpoth et al. 1999). Thus, the homologous G_α subunits appear to exert opposite regulatory effects by binding to pseudo dyad-related sites on the intramolecular, heterodimeric mammalian C_1-C_2 heterodimers (Fig. 9a). Experiments with extended constructs indicate that regions outside of the C_1 CHD domain are also involved in the interaction with $G\alpha_i$ (Dessauer et al. 1998). As $G\alpha_i$ is a noncompetitive inhibitor of $G\alpha_s$ -stimulated AC, it is probable that $G\alpha_i$ binds directly to the $G\alpha_s$-bound AC complex. The structural mechanism of inhibition is unknown. However, it has not been possible to isolate a ternary complex between $G\alpha_i$, $G\alpha_s$, and isolated C_1 and C_2 domains (Dessauer et al. 1998). Therefore it is possible that $G\alpha_i$ weakens the C_1-C_2 interface and prevents essential conformational changes in regions key to catalysis. Since C_1-C_2 heterodimers have been captured only in $G\alpha_s$- and forskolin-activated states, the basal, ligand-free state of the C_1-C_2 heterodimers, and consequently, the changes wrought by their regulators, cannot be accurately defined. Further, it is probable that, like $G\alpha_i$, other regulators of mACs such as Gβγ, calmodulin kinase II, and protein kinase C, that act chiefly on the $G\alpha_s$-stimulated state of ACs, also function by regulating conformational changes at the domain interface. Unlike the pseudo dyad-related binding sites of the

Fig. 9 Regulation and conformational change in the mammalian mACs. **a** Asymmetric regulation of the VC_1-IIC_2 heterodimer by $G\alpha_s$. VC_1, IIC_2, and $G\alpha_s$ are colored *salmon*, *green*, and *violet*, respectively. Molecular details of the substrate analog ATPαS and the activator forskolin bound to the VC_1-IIC_2 heterodimer and the GTP analog bound to $G\alpha_s$ are shown. Selected structural elements of VC_1-IIC_2 and the switch II helix of $G\alpha_s$ are labeled. **b** Conformational change in the $G\alpha_s$ and forskolin-activated VC_1-IIC_2 heterodimer upon binding of substrate. VC_1 and IIC_2 subunits are colored *khaki* and *gray*, respectively, in the "open" state crystallized in the absence of substrate, and *green* and *salmon*, respectively, in the presence of ATPαS; $G\alpha_s$, forskolin, and ATPαS are not shown. Secondary structure elements, β1-α1-α2 segment of VC_1 and β6-β7 hairpin of IIC_2, which show the largest displacements upon binding of ATPαS, are indicated ▶

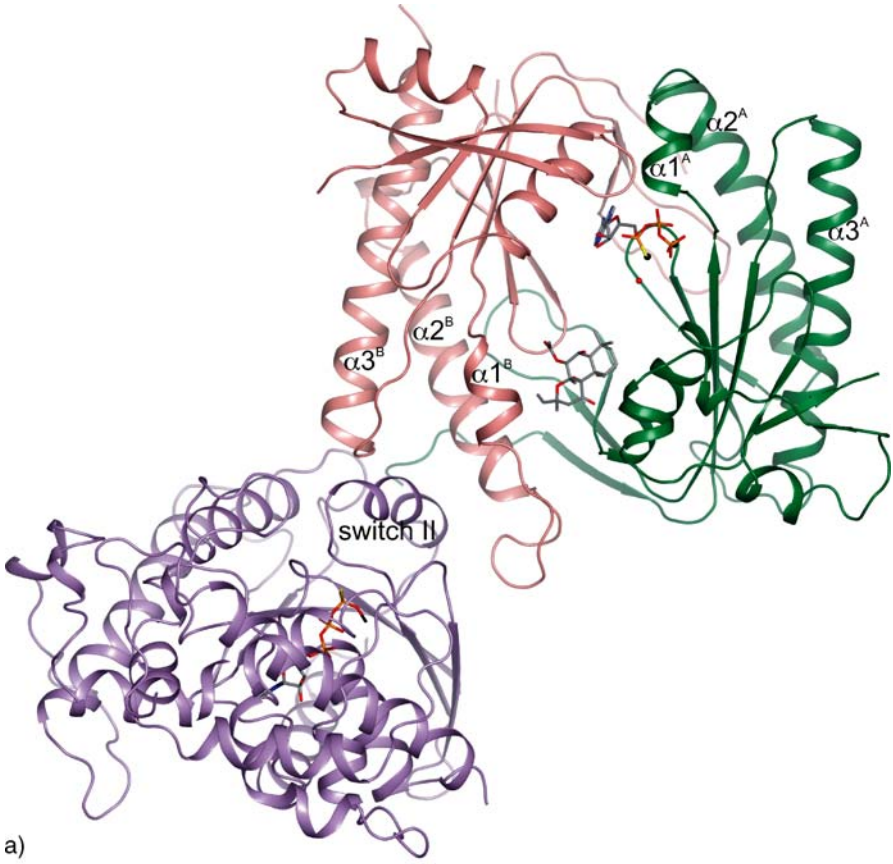

a)

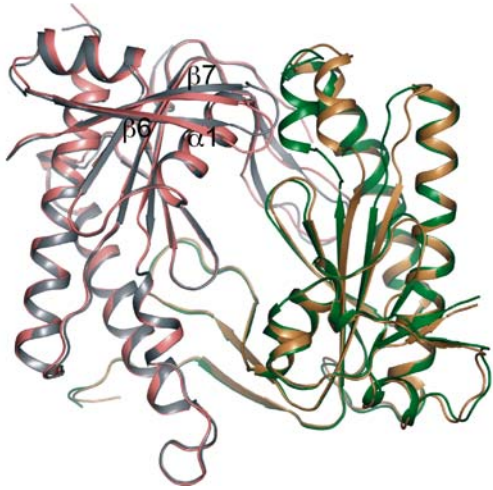

b)

homologous $G\alpha_s$ and $G\alpha_i$ subunits, these regulators are expected to bind asymmetrically to C_1-C_2 heterodimer. The diterpene forskolin, a nonphysiological activator of most of the mammalian mACs, appears to stabilize both a productive C_1-C_2 heterodimer as well as catalytically competent conformations of loops and residues involved in catalysis, playing a role similar to $G\alpha_s$. Forskolin binds to a site related to the heterodimer active site by the pseudo-dyad axis, raising the tantalizing possibility that this might constitute the binding site of an as-yet-unidentified, physiologically relevant, small-molecule regulator of mammalian mAC heterodimers (Fig. 9a).

Structures of the soluble *S. platensis* CyaC captured in complex with the substrate analogs AMPCPP and ATPαS suggest mechanisms by which small-molecule regulators may directly regulate CHD enzyme activity. *S. platensis* CyaC serves as a model for the mammalian sAC as both these enzymes are synergistically activated by Ca^{2+} and bicarbonate (Steegborn et al. 2005b). Further, catechol estrogens, which are formed by the oxidative hydroxylation of the steroid estrogen, are physiologically relevant, noncompetitive inhibitors of both mammalian sAC and mACs and also inhibit *S. platensis* CyaC in a similar manner (Steegborn et al. 2005a). Interestingly Ca^{2+} activates *S. platensis* CyaC and the mammalian sAC (Cann et al. 2003; Chen et al. 2000; Hyne and Garbers 1979; Jaiswal and Conti 2003; Litvin et al. 2003), but inhibits activity of the type V mACs (Hu et al. 2002), although it appears to bind to the B-metal site of both these enzymes (Steegborn et al. 2005b; T.-C. Mou, unpublished). The reason for these contradictory effects is unclear. Perhaps Ca^{2+} better stabilizes polyphosphate in both enzymes, facilitating binding of substrate, but in the type V mAC it also results in the product pyrophosphate being bound too tightly, inhibiting product release and consequently enzyme activity. In solution, bicarbonate activates these sACs and this activation does not appear to be a pH-mediated effect. Flash-soaking bicarbonate into substrate analog-bound crystals of CyaC resulted in conformational changes in the α1-helix and β6-β7 loop, resulting in the formation of a more closed dimer. However, no electron density was observed for the bicarbonate, and therefore its binding site could not be identified. Similar conformational changes were seen upon binding ATPαS, suggesting either that potent substrate analogs and bicarbonate drive the enzyme to the same conformational state or that the full repertoire of conformational changes effected by bicarbonate are not observed in the crystal structures so far determined. Thus, the mechanism by which bicarbonate and Ca^{2+} alone activate CyaC is not completely clear.

The probable mechanism by which catechol estrogens inhibit sACs was suggested by the structure of CyaC in complex with AMPCPP, the catechol estrogens, and two metal cations (Steegborn et al. 2005a). The catechol estrogen binds at a site adjacent to the CHD active site, in a hydrophobic pocket formed by residues from α4 and β1 of one CHD and the β2-β3 hairpin of both CHDs. The hydroxyls of the catechol estrogen hydroxyls chelate and displace the A-site metal from its normal position, presumably aborting catalysis. Further, AMPCPP is displaced such that its adenine is no longer within hydrogen-bonding distance of the dimerization arm^B Thr^B, and the α- and β-phosphates occupy positions typically occupied by the β- and γ-phosphates, respectively. *S. platensis* CyaC is a symmetrical, homodimeric enzyme (Fig. 8a), and regulatory molecules such as catechol estrogen and Ca^{2+} are identically bound to symmetrical dyad-related sites. Unlike the homodimer CyaC, however, the tandem CHDs of the soluble mammalian AC are not identical in sequence, and consequently the catalytic dimer formed by these domains must be pseudosymmetrical. Substitution of one of the two conserved catalytic aspartate residues in the C_1 domain by cysteine, and an insertion of several residues in the $\beta2^A$-$\beta3^A$ hairpin suggests that mammalian sAC possesses only one functional catalytic site. It is therefore possible that the asymmetry of

the mammalian sAC will also be reflected in the mechanism of its regulation, reminiscent of the mammalian mACs.

M. tuberculosis Rv1900c is a two-domain, homodimeric MNC. The N-terminal domain bears sequence similarity to members of the α/β hydrolase family of lipases but has no catalytic activity toward known substrates, and appears to have weak, negative regulatory activity (Sinha et al. 2005). The C-terminal CHD, upon homodimerization, can use both ATP and GTP as substrate but has a 14-fold preference for ATP. Structures of Rv1900c CHD homodimers with and without the substrate analog AMPCPP demonstrated that even in the absence of additional regulatory stimuli, binding of substrate induces conformational changes within each CHD accompanied by a dramatic rotation of 16.6° and translation of 11 Å of the CHDs relative to each other, to form a catalytically competent dimer (Fig. 10a). As discussed previously, the Rv1900c CHD homodimers are structurally and mechanistically asymmetrical in both open and closed states. The role of the Rv1900c N-terminal regulatory domain in the regulation of the transition between inactive, open and the active, closed dimers, its influence on the structural and mechanistic asymmetry observed in the isolated Rv1900c CHD homodimers, and its effect upon substrate specificity has not yet been established.

M. tuberculosis Rv1264 is a two-domain AC comprising an N-terminal, 10-helix regulatory domain and a C-terminal CHD that also functions as a homodimer (Linder et al. 2002). Rv1264 is a pH-regulated enzyme that presumably plays a role in mycobacterial survival in the acidic environment of the phagolysosome. In the activated state, and even in the absence of substrate, the two CHDs form a homodimer whose subunits are arranged in a closed conformation similar to that seen in the ligand-bound structures of other CHDs (Fig. 10b; Tews et al. 2005). This active homodimer contains two identical, symmetrical active sites, each of which contains a complete, appropriately located complement of residues required for

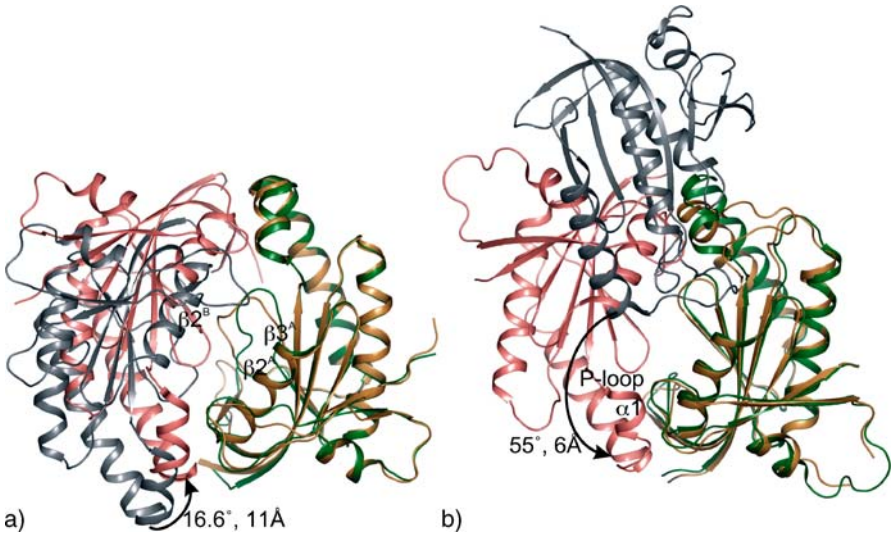

Fig. 10a, b Conformational change in two mycobacterial NCs. CHDs are colored *gray* and *khaki* in the open, catalytically incompetent conformation, and *salmon* and *green* in the closed, catalytically competent, conformation. The movement of the CHDs constituting a dimer, relative to each other, as well as the secondary structure elements that undergo the largest conformational changes are indicated. **a** Conformational change in Rv1900c CHD homodimers upon binding of substrate. The change from an open to a closed state is triggered by binding of the ATP analog, AMPCPP. **b** Conformational change in Rv1264 CHD dimers upon activation by pH

catalysis. Structures of the Rv1264 holoprotein crystallized at neutral and acidic pH demonstrate that CHD activity is also regulated by dramatic conformational changes, wherein the α1-helix of the CHD unfolds, destroying the ATP phosphate-binding subsite; concomitantly, the active sites of the dimer are disassembled by a dramatic rotation of 55° and translation of 6 Å of the two CHDs relative to each other (Fig. 10b; Tews et al. 2005). The regulatory domain of each subunit of the homodimer makes extensive contacts with the CHD of the other in both active and inactive states, and the pH-triggered inactivating transformation is effected by the pH-dependent extension of the C-terminal helix of the regulatory domain by four turns (Fig. 11). Despite these large conformational changes, in both active and inactive states, Rv1264 forms symmetrical homodimers and the regulatory domains from each of the two subunits that constitute the homodimer make identical, symmetrical contacts with the trans CHD (Fig. 11).

Like the prokaryotic CHDs, GGDEF domains appear to be covalently linked to a wide range of sensory/regulatory domains, but very little is known about the mechanism by which these domains regulate DGC activity. However, it appears that like the CHDs, regulating the formation of catalytically competent GGDEF domain dimers may be a key mode of regulation in DGCs. *C. crescentus* PleD, the only DGC of known structure, contains a CheY-like receiver domain a second CheY-like adaptor domain, in addition to the GGDEF domain (Chan et al. 2004). The structure of the nonphosphorylated form of the molecule provides clues to the mechanism by which activity of PleD is regulated (Chan et al. 2004). Inactivate PleD appears to be a monomer in solution. The sensor histidine kinase phosphorylates a receiver domain aspartate located at the interface of the receiver and adaptor domains, which is predicted to induce repacking of this interface and subsequent reorientation of the receiver and adaptor domains relative to each other. In this activated orientation, the receiver domain of one DGC can form isologous contacts with the adaptor domain of another activated DGC, enhancing formation of a catalytically competent GGDEF domain homodimer. In addition to regulation by the CheY-like domains, PleD is subject to tight feedback inhibition by the product c-diGMP. Two c-diGMP molecules with mutually intercalated purine bases bind as a single unit at a site distant from the GGDEF domain active site, located at the interface between the GGDEF domain and the CheY-like adaptor domain. Binding at this site has been proposed to stabilize the GGDEF domain-adaptor domain interface in an inactive state that hampers the formation of catalytically competent GGDEF domain homodimers. Thus, binding of the product, c-diGMP, to this inhibitory site enables noncompetitive, allosteric, feedback inhibition that overrides the stimulus-driven upregulation of DGC activity by the CheY-like regulatory domains.

It is clear that class III NCs are regulated by diverse mechanisms. Despite variability in the mode of regulation, current evidence suggests that most regulatory mechanisms involve formation or dissolution of catalytically competent active sites, effected by rearrangement of the two catalytic domains of the dimer relative to each other as well as the conformational changes in active site loops. In general, there appears to be an inverse correlation between the diversity in the architecture of the class III NCs and the complexity of signaling pathways that interact with them. Thus, NCs from lower organisms that are active as intermolecular homodimers show greater variation in architecture, enabling the different NCs to respond directly to different stimuli. In contrast, MNCs from higher organisms have a more uniform architecture, possibly having evolved by gene duplication of a primitive CHD to form intramolecular CHD heterodimers. The emergence of more complex regulatory networks accompanied the divergence of the duplicated genes and the subsequent pseudo-symmetry inherent in the heterodimers. These features have enabled MNCs to serve as integration points for networks of signaling pathways.

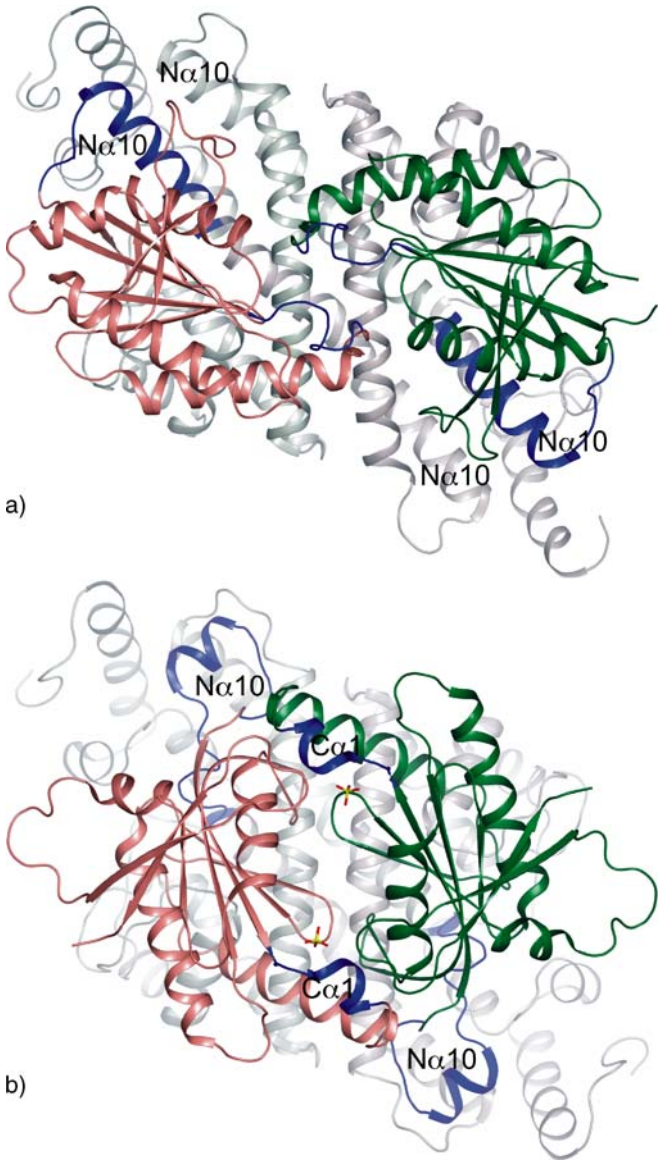

Fig. 11a, b pH-triggered conformational change and regulation of Rv1264. The subunits are colored *green* and *salmon*, with the regulatory domain of each subunit overlaid with *gray*. Secondary structure elements that undergo dramatic conformational changes are labeled and highlighted in *blue*. **a** The open, catalytically incompetent conformation. The C-terminal helix (*Nα10*) of each N-terminal, regulatory domain is elongated by four turns (colored *blue*). The P-loop and the α1 helix of each CHD (also colored *blue*) are unfolded. **b** The closed, catalytically competent conformation. The last four turns of Nα10 unfold and are rearranged. The P-loop and the α1 helix (labeled Cα1, colored *blue*) of each CHD fold into conformations similar to that seen in other CHD structures. A sulfate molecule bound in the polyphosphate-binding site is depicted in molecular detail

Nearly a decade has passed since the structures of the mammalian AC catalytic modules were first published, during which the catalog of eukaryotic NCs appears to have been nearly completed and the major pathways by which they are regulated well-delineated. However, it is clear that the molecular basis of the regulatory complexity of this family of enzymes has yet to be fully explored. In contrast to eukaryotic class III MNCs, a plethora of prokaryotic enzymes have been identified from the genomic sequences of prokaryotic organisms, and the divergent domain structure of these proteins suggests new modes of regulation. Thus, efforts to understand the regulatory mechanisms of the class III NCs in molecular detail shall continue to pose substantial experimental challenges in the years to come.

Acknowledgements. We acknowledge support from the Howard Hughes Medical Institute, NIH grant DK46371 (SRS), Welch Foundation grant I-1229 (SRS) and the John W. and Rhonda K. Pate Professorship to SRS.

References

Artymiuk PJ, Poirette AR, Rice DW, Willett P (1997) A polymerase I palm in adenylyl cyclase? Nature 388:33–34

Barton GJ (1993) ALSCRIPT: a tool to format multiple sequence alignments. Protein Eng 6:37–40

Barzu O, Danchin A (1994) Adenylyl cyclases: a heterogeneous class of ATP-utilizing enzymes. Prog Nucleic Acid Res Mol Biol 49:241–283

Beese LS, Steitz TA (1991) Structural basis for the 3′-5′ exonuclease activity of *Escherichia coli* DNA polymerase I: a two metal ion mechanism. EMBO J 10:25–33

Beuve A (1999) Conversion of a guanylyl cyclase to an adenylyl cyclase. Methods 19:545–550

Beuve A, Krin E, Danchin A (1993) *Rhizobium meliloti* adenylate cyclase: probing of a NTP-binding site common to cyclases and cation transporters. C R Acad Sci III 316:533–539

Bieger B, Essen LO (2001) Structural analysis of adenylate cyclases from *Trypanosoma brucei* in their monomeric state. EMBO J 20:433–445

Brautigam CA, Steitz TA (1998) Structural and functional insights provided by crystal structures of DNA polymerases and their substrate complexes. Curr Opin Struct Biol 8:54–63

Buck J, Sinclair ML, Schapal L, Cann MJ, Levin LR (1999) Cytosolic adenylyl cyclase defines a unique signaling molecule in mammals. Proc Natl Acad Sci USA 96:79–84

Cann MJ, Hammer A, Zhou J, Kanacher T (2003) A defined subset of adenylyl cyclases is regulated by bicarbonate ion. J Biol Chem 278:35033–35038

Chan C, Paul R, Samoray D, Amiot NC, Giese B, Jenal U, Schirmer T (2004) Structural basis of activity and allosteric control of diguanylate cyclase. Proc Natl Acad Sci USA 101:17084–17089

Chen Y, Weng G, Li J, Harry A, Pieroni J, Dingus J, Hildebrandt JD, Guarnieri F, Weinstein H, Iyengar R (1997) A surface on the G protein beta-subunit involved in interactions with adenylyl cyclases. Proc Natl Acad Sci USA 94:2711–2714

Chen Y, Cann MJ, Litvin TN, Iourgenko V, Sinclair ML, Levin LR, Buck J (2000) Soluble adenylyl cyclase as an evolutionarily conserved bicarbonate sensor. Science 289:625–628

Cooper D (2005) Compartmentalization of adenylate cyclase and cAMP signalling. Biochem Soc Trans 33:1319–1322

Cooper DM, Mons N, Fagan K (1994) Ca(2+)-sensitive adenylyl cyclases. Cell Signal 6:823–840

Cooper DM, Mons N, Karpen JW (1995) Adenylyl cyclases and the interaction between calcium and cAMP signalling. Nature 374:421–424

Cooper DM, Schell MJ, Thorn P, Irvine RF (1998) Regulation of adenylyl cyclase by membrane potential. J Biol Chem 273:27703–27707

Cooper DMF (2003) Regulation and organization of adenylyl cyclases and cAMP. Biochem J 375:517–529

Cotta M, Whitehead T, Wheeler M (1998) Identification of a novel adenylate cyclase in the ruminal anaerobe, *Prevotella ruminicola* D31d. FEMS Microbiol Lett 164:257–260

Coudart-Cavalli MP, Sismeiro O, Danchin A (1997) Bifunctional structure of two adenylyl cyclases from the myxobacterium *Stigmatella aurantiaca*. Biochimie 79:757–767

Dessauer CW, Gilman AG (1997) The catalytic mechanism of mammalian adenylyl cyclase. Equilibrium binding and kinetic analysis of P-site inhibition. J Biol Chem 272:27787–27795

Dessauer CW, Scully TT, Gilman AG (1997) Interactions of forskolin and ATP with the cytosolic domains of mammalian adenylyl cyclase. J Biol Chem 272:22272–22277
Dessauer CW, Tesmer JJ, Sprang SR, Gilman AG (1998) Identification of a Gia binding site on type V adenylyl cyclase. J Biol Chem 273:25831–25839
Dessauer CW, Tesmer JJ, Sprang SR, Gilman AG (1999) The interactions of adenylate cyclases with P-site inhibitors. Trends Pharmacol Sci 20:205–210
Doublié S, Ellenberger T (1998) The mechanism of action of T7 DNA polymerase. Curr Opin Struct Biol 8:704–712
Drum CL, Yan SZ, Bard J, Shen YQ, Lu D, Soelaiman S, Grabarek Z, Bohm A, Tang WJ (2002) Structural basis for the activation of anthrax adenylyl cyclase exotoxin by calmodulin. Nature 415:396–402
Eckstein F, Romaniuk PJ, Heideman W, Storm DR (1981) Stereochemistry of the mammalian adenylate cyclase reaction. J Biol Chem 256:9118–9120
Feng Q, Zhang Y, Li Y, Liu Z, Zuo J, Fang F (2005) Two domains are critical for the nuclear localization of soluble adenylyl cyclase. Biochimie 88:319–328
Gallagher DT, Smith NN, Kim SK, Heroux A, Robinson H, Reddy PT (2006) Structure of the Class IV Adenylyl Cyclase Reveals a Novel Fold. J Mol Biol. 2006 Aug 11; [Epub ahead of print]
Geng W, Wang Z, Zhang J, Reed BY, Pak CYC, Moe OW (2005) Cloning and characterization of the human soluble adenylyl cyclase. Am J Physiol Cell Physiol 288:C1305–1316
Gu C, Cali JJ, Cooper DM (2002) Dimerization of mammalian adenylate cyclases. Eur J Biochem 269:413–421
Guo Q, Shen Y, Zhukovskaya NL, Florian J, Tang WJ (2004) Structural and kinetic analyses of the interaction of anthrax adenylyl cyclase toxin with reaction products cAMP and pyrophosphate. J Biol Chem 279:29427–29435
Guo Q, Shen Y, Lee YS, Gibbs CS, Mrksich M, Tang WJ (2005) Structural basis for the interaction of *Bordetella pertussis* adenylyl cyclase toxin with calmodulin. EMBO J 24:3190–3201
Guo YL, Seebacher T, Kurz U, Linder JU, Schultz JE (2001) Adenylyl cyclase Rv1625c of *Mycobacterium tuberculosis*: a progenitor of mammalian adenylyl cyclases. EMBO J 20:3667–3675
Hanoune J, Defer N (2001) Regulation and role of adenylyl cyclase isoforms. Annu Rev Pharmacol Toxicol 41:145–174
Holland MM, Leib TK, Gerlt JA (1988) Isolation and characterization of a small catalytic domain released from the adenylate cyclase from *Escherichia coli* by digestion with trypsin. J Biol Chem 263:14661–14668
Hu B, Nakata H, Gu C, De Beer T, Cooper DM (2002) A critical interplay between Ca^{2+} inhibition and activation by Mg^{2+} of AC5 revealed by mutants and chimeric constructs. J Biol Chem 277:33139–33147
Hurley J (1998) The adenylyl and guanylyl cyclase superfamily. Curr Opin Struct Biol 8:770–777
Hurley JH (1999) Structure, mechanism, and regulation of mammalian adenylyl cyclase. J Biol Chem 274:7599–7602
Hyne RV, Garbers DL (1979) Regulation of guinea pig sperm adenylate cyclase by calcium. Biol Reprod 21:1135–1142
Jaiswal BS, Conti M (2001) Identification and functional analysis of splice variants of the germ cell soluble adenylyl cyclase. J Biol Chem 276:31698–31708
Jaiswal BS, Conti M (2003) Calcium regulation of the soluble adenylyl cyclase expressed in mammalian spermatozoa. Proc Natl Acad Sci USA 100:10676–10681
Kasahara M, Unno T, Yashiro K, Ohmori M (2001) CyaG, a novel cyanobacterial adenylyl cyclase and a possible ancestor of mammalian guanylyl cyclases. J Biol Chem 276:10564–10569
Ketkar A, Shenoya A, Ramagopal UA, Visweswariaha SS, Sugun K (2006) A structural basis for the role of nucleotide specifying residues in regulating the oligomerization of the Rv1625c adenylyl cyclase from M. tuberculosis. J Mol Biol 356:904–916
Ketkar AD, Shenoy AR, Kesavulu MM, Visweswariah SS, Suguna K (2004) Purification, crystallization and preliminary X-ray diffraction analysis of the catalytic domain of adenylyl cyclase Rv1625c from *Mycobacterium tuberculosis*. Acta Crystallogr D Biol Crystallogr 60:371–373
Kimura Y, Vassylyev DG, Matsushima M, Mitsuoka K, Murata K, Hiral T, Fujiyoshi Y (1997) Surface of bacteriorhodopsin revealed by high-resolution electron crystallography. Nature 389:206–211
Krupinski J, Cali JJ (1998) Molecular diversity of the adenylyl cyclases. Adv Second Messenger Phosphoprotein Res 32:53–79
Ladant D, Ullmann A (1999) *Bordetella pertussis* adenylate cyclase: a toxin with multiple talents. Trends Microbiol 7:172–176
Leppla SH (1982) Anthrax toxin edema factor: a bacterial adenylate cyclase that increases cyclic AMP concentrations of eukaryotic cells. Proc Natl Acad Sci USA 79:3162–3166

Linder JU (2005) Substrate selection by class III adenylyl cyclases and guanylyl cyclases. IUBMB Life 57:797–803
Linder JU, Schultz JE (2003) The class III adenylyl cyclases: multi-purpose signalling modules. Cell Signal 15:1081–1089
Linder JU, Engel P, Reimer A, Kruger T, Plattner H, Schultz A, Schultz JE (1999) Guanylyl cyclases with the topology of mammalian adenylyl cyclases and an N-terminal P-type ATPase-like domain in Paramecium, Tetrahymena and Plasmodium. EMBO J 18:4222–4232
Linder JU, Hoffmann T, Kurz U, Schultz JE (2000) A guanylyl cyclase from Paramecium with 22 transmembrane spans. Expression of the catalytic domains and formation of chimeras with the catalytic domains of mammalian adenylyl cyclases. J Biol Chem 275:11235–11240
Linder JU, Schultz A, Schultz JE (2002) Adenylyl cyclase Rv1264 from *Mycobacterium tuberculosis* has an autoinhibitory N-terminal domain. J Biol Chem 277:15271–15276
Linder JU, Hammer A, Schultz JE (2004) The effect of HAMP domains on class IIIb adenylyl cyclases from *Mycobacterium tuberculosis*. Eur J Biochem 271:2446–2451
Litvin NT, Kamenetsky M, Zarifyan A, Buck J, Levin LR (2003) Kinetic properties of "soluble" adenylyl cyclase. Synergism between calcium and bicarbonate. J Biol Chem 278:15922–15926
Liu Y, Ruoho AE, Rao VD, Hurley JH (1997) Catalytic mechanism of the adenylyl and guanylyl cyclases: modeling and mutational analysis. Proc Natl Acad Sci USA 94:13414–13419
Masuda S, Ono TA (2005) Adenylyl cyclase activity of Cya1 from the cyanobacterium *Synechocystis* sp. strain PCC 6803 is inhibited by bicarbonate. J Bacteriol 187:5032–5035
McCue LA, McDonough KA, Lawrence CE (2000) Functional classification of cNMP-binding proteins and nucleotide cyclases with implications for novel regulatory pathways in *Mycobacterium tuberculosis*. Genome Res 10:204–219
Mons N, Decorte L, Jaffard R, Cooper DM (1998) Ca^{2+}-sensitive adenylyl cyclases, key integrators of cellular signalling. Life Sci 62:1647–1652
Mou TC, Gille A, Fancy DA, Seifert R, Sprang SR (2005) Structural basis for the inhibition of mammalian membrane adenylyl cyclase by 2′(3′)-O-(N-methylanthraniloyl)-guanosine 5′-triphosphate. J Biol Chem 280:7253–7261
Murzin AG (1998) How far divergent evolution goes in proteins. Curr Opin Struct Biol 8:380–387
Noyama K, Maekawa S (2003) Localization of cyclic nucleotide phosphodiesterase 2 in the brain-derived Triton-insoluble low-density fraction (raft). Neurosci Res 45:141–148
Ochoa de Alda JAG, Ajlani G, Houmard J (2000) *Synechocystis* strain PCC 6803 cya2, a prokaryotic gene that encodes a guanylyl cyclase. J Bacteriol 182:3839–3842
Pei J, Grishin N (2001) GGDEF domain is homologous to adenylyl cyclase. Proteins 42:210–216
Reddy P, Hoskins J, McKenney K (1995a) Mapping domains in proteins: dissection and expression of *Escherichia coli* adenylyl cyclase. Anal Biochem 231:282–286
Reddy R, Smith D, Wayman G, Wu Z, Villacres EC, Storm DR (1995b) Voltage-sensitive adenylyl cyclase activity in cultured neurons. A calcium-independent phenomenon. J Biol Chem 270:14340–14346
Roelofs J, Van Haastert PJM (2002) Deducing the origin of soluble adenylyl cyclase, a gene lost in multiple lineages. Mol Biol Evol 19:2239–2246
Romling U, Gomelsky M, Galperin MY (2005) C-di-GMP: the dawning of a novel bacterial signalling system. Mol Microbiol 57:629–639
Scholich K, Barbier AJ, Mullenix JB, Patel TB (1997a) Characterization of soluble forms of nonchimeric type V adenylyl cyclase. Proc Natl Acad Sci USA 94:2915–2920
Scholich K, Wittpoth C, Barbier AJ, Mullenix JB, Patel TB (1997b) Identification of an intramolecular interaction between small regions in type V adenylyl cyclase that influences stimulation of enzyme activity by Gsalpha. Proc Natl Acad Sci USA 94:9602–9607
Seebacher T, Linder JU, Schultz JE (2001) An isoform-specific interaction of the membrane anchors affects mammalian adenylyl cyclase type V activity. Eur J Biochem 268:105–110
Shen Y, Zhukovskaya NL, Guo Q, Florián J, Tang WJ (2005) Calcium-independent calmodulin binding and two-metal-ion catalytic mechanism of anthrax edema factor. EMBO J 24:929–941
Shenoy A, Visweswariah S (2004) Class III nucleotide cyclases in bacteria and archaebacteria: lineage-specific expansion of adenylyl cyclases and a dearth of guanylyl cyclases. FEBS Lett 561:11–21
Shenoy AR, Srinivasan N, Subramaniam M, Visweswariah SS (2003) Mutational analysis of the *Mycobacterium tuberculosis* Rv1625c adenylyl cyclase: residues that confer nucleotide specificity contribute to dimerization. FEBS Lett 545:253–259
Shenoy AR, Sreenath NP, Mahalingam M, Visweswariah SS (2005) Characterization of phylogenetically distant members of the adenylate cyclase family from mycobacteria: Rv1647 from *Mycobacterium tuberculosis* and its orthologue ML1399 from M. leprae. Biochem J 387:541–551
Simonds WF (1999) G protein regulation of adenylate cyclase. Trends Pharmacol Sci 20:66–73

Sinha SC, Wetterer M, Sprang SR, Schultz JE, Linder JU (2005) Origin of asymmetry in adenylyl cyclases: structures of *Mycobacterium tuberculosis* Rv1900c. EMBO J 24:663–673
Sismeiro O, Trotot P, Biville F, Vivares C, Danchin A (1998) *Aeromonas hydrophila* adenylyl cyclase2: a new class of adenylyl cyclases with thermophilic properties and sequence similarities to proteins from hyperthermophilic archaebacteria. J Bacteriol 180:3339–3344
Smit MJ, Iyengar R (1998) Mammalian adenylyl cyclases. Adv Second Messenger Phosphoprotein Res 32:1–21
Steegborn C, Litvin TN, Hess KC, Capper AB, Taussig R, Buck J, Levin LR, Wu H (2005a) A novel mechanism for adenylyl cyclase inhibition from the crystal structure of its complex with catechol estrogen. J Biol Chem 280:31754–31759
Steegborn C, Litvin TN, Levin LR, Buck J, Wu H (2005b) Bicarbonate activation of adenylyl cyclase via promotion of catalytic active site closure and metal recruitment. Nat Struct Mol Biol 12:32–37
Steitz TA (1993) DNA- and RNA-dependent DNA polymerases. Curr Opin Struct Biol 3:31–38
Steitz TA (1999) DNA polymerases: structural diversity and common mechanisms. J Biol Chem 274:17395–17398
Steitz TA, Steitz JA (1993) A general two-metal-ion mechanism for catalytic RNA. Proc Natl Acad Sci USA 90:6498–6502
Steitz TA, Smerdon SJ, Jäger J, Joyce CM (1994) A unified polymerase mechanism for nonhomologous DNA and RNA polymerases. Science 266:2022–2025
Süsstrunk U, Pidoux J, Taubert S, Ullmann A, CJ T (1998) Pleiotropic effects of cAMP on germination, antibiotic biosynthesis and morphological development in *Streptomyces coelicolor*. Mol Microbiol 30:33–46
Sunahara RK, Taussig R (2002) Isoforms of mammalian adenylyl cyclase: multiplicities of signaling. Mol Interv 2:168–184
Sunahara RK, Dessauer CW, Gilman AG (1996) Complexity and diversity of mammalian adenylyl cyclases. Annu Rev Pharmacol Toxicol 36:461–480
Sunahara RK, Dessauer CW, Whisnant RE, Kleuss C, Gilman AG (1997) Interaction of Gsa with the cytosolic domains of mammalian adenylyl cyclase. J Biol Chem 272:22265–22271
Sunahara RK, Beuve A, Tesmer JJG, Sprang SR, Garbers DL, Gilman AG (1998) Exchange of substrate and inhibitor specificities between adenylyl and guanylyl cyclases. J Biol Chem 273:16332–16338
Tang WJ, Gilman AG (1995) Construction of a soluble adenylyl cyclase activated by Gs alpha and forskolin. Science 268:1769–1772
Tang WJ, Stanzel M, Gilman AG (1995) Truncation and alanine-scanning mutants of type I adenylyl cyclase. Biochemistry 34:14563–14572
Tang WJ, Yan S, Drum CL (1998) Class III adenylyl cyclases: regulation and underlying mechanisms. Adv Second Messenger Phosphoprotein Res 32:137–151
Taussig R, Zimmermann G (1998) Type-specific regulation of mammalian adenylyl cyclases by G protein pathways. Adv Second Messenger Phosphoprotein Res 32:81–98
Taussig R, Iniguez-Lluhi JA, Gilman AG (1993) Inhibition of adenylyl cyclase by Gi alpha. Science 261:218–221
Taussig R, Tang WJ, Hepler JR, Gilman AG (1994) Distinct patterns of bidirectional regulation of mammalian adenylyl cyclases. J Biol Chem 269:6093–6100
Tellez-Sosa J, Soberon N, Vega-Segura A, Torres-Marquez ME, Cevallos MA (2002) The rhizobium etli cyaC product: characterization of a novel adenylate cyclase class. J Bacteriol 184:3560–3568
Tesmer JJ, Sprang SR (1998) The structure, catalytic mechanism and regulation of adenylyl cyclase. Curr Opin Struct Biol 8:713–719
Tesmer JJ, Dessauer CW, Sunahara RK, Murray LD, Johnson RA, Gilman AG, Sprang SR (2000) Molecular basis for P-site inhibition of adenylyl cyclase. Biochemistry 39:14464–14471
Tesmer JJG, Sunahara RK, Gilman AG, Sprang SR (1997) Crystal structure of the catalytic domains of adenylyl cyclase in a complex with Gsa_GTPgS. Science 278:1907–1916
Tesmer JJG, Sunahara RK, Johnson RA, Gilman AG, Sprang SR (1999) Two metal ion catalysis in adenylyl cyclase. Science 285:756–760
Tews I, Findeisen F, Sinning I, Schultz A, Schultz JE, Linder JU (2005) The structure of a pH-sensing mycobacterial adenylyl cyclase holoenzyme. Science 308:1020–1023
Tucker CL, Hurley JH, Miller TR, Hurley JB (1998) Two amino acid substitutions convert a guanylyl cyclase, RetGC-1, into an adenylyl cyclase. Proc Natl Acad Sci USA 95:5993–5997
Weber JH, Vishnyakov A, Hambach K, Schultz A, Schultz JE, Linder JU (2004) Adenylyl cyclases from plasmodium, paramecium and tetrahymena are novel ion channel/enzyme fusion proteins. Cell Signal 16:115–125

Whisnant RE, Gilman AG, Dessauer CW (1996) Interaction of the two cytosolic domains of mammalian adenylyl cyclase. Proc Natl Acad Sci USA 93:6621–6625

Wittpoth C, Scholich K, Yigzaw Y, Stringfield TM, Patel TB (1999) Regions on adenylyl cyclase that are necessary for inhibition of activity by beta gamma and G(ialpha) subunits of heterotrimeric G proteins. Proc Natl Acad Sci USA 96:9551–9556

Yahr TL, Vallis AJ, Hancock MK, Barbieri JT, Frank DW (1998) ExoY, an adenylate cyclase secreted by the *Pseudomonas aeruginosa* type III system. Proc Natl Acad Sci USA 95:13899–13904

Yan SZ, Hahn D, Huang ZH, Tang WJ (1996) Two cytoplasmic domains of mammalian adenylyl cyclase form a Gsa- and forskolin-activated enzyme in vitro. J Biol Chem 271:10941–10945

Yan SZ, Huang ZH, Rao VD, Hurley JH, Tang WJ (1997a) Three discrete regions of mammalian adenylyl cyclase form a site for Gsalpha activation. J Biol Chem 272:18849–18854

Yan SZ, Huang ZH, Shaw RS, Tang WJ (1997b) The conserved asparagine and arginine are essential for catalysis of mammalian adenylyl cyclase. J Biol Chem 272:12342–12349

Zehmer JK, Hazel JR (2003) Plasma membrane rafts of rainbow trout are subject to thermal acclimation. J Exp Biol 206:1657–1667

Zhang G, Liu Y, Ruoho AE, Hurley JH (1997) Structure of the adenylyl cyclase catalytic core. Nature 386:247–253

Zimmermann G, Zhou D, Taussig R (1998) Mutations uncover a role for two magnesium ions in the catalytic mechanism of adenylyl cyclase. J Biol Chem 273:19650–19655